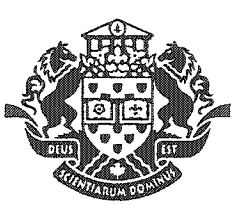

Université d'Ottawa · University of Ottawa

Université d'Ottawa · University of Ottawa

FACULTÉ DES ÉTUDES SUPÉRIEURES ET POSTDOCTORALES

FACULTY OF GRADUATE AND POSTDOCTORAL STUDIES

GANGARAJU, Sandhya

AUTEUR DE LA THÈSE - AUTHOR OF THESIS

M.Sc. (Biochemistry)

GRADE - DEGREE

Biochemistry, Microbiology and Immunology

FACULTÉ, ÉCOLE, DÉPARTEMENT - FACULTY, SCHOOL, DEPARTMENT

TITRE DE LA THÈSE - TITLE OF THE THESIS

Role of Mitofusin2 in the Regulation of Mitochondrial Dynamics

H. McBride

DIRECTEUR DE LA THÈSE - THESIS SUPERVISOR

EXAMINATEURS DE LA THÈSE - THESIS EXAMINERS

D. Franks

M. Hefford

J.-M. De Koninck, Ph.D.

LE DOYEN DE LA FACULTÉ DES ÉTUDES SUPÉRIEURES ET POSTDOCTORALES

SIGNATURE

DEAN OF THE FACULTY OF GRADUATE AND POSTDOCTORAL STUDIES

Role of Mitofusin2 in the Regulation of Mitochondrial Dynamics

SANDHYA GANGARAJU

Thesis submitted to the
Faculty of Graduate and Postdoctoral Studies
in partial fulfillment of the requirements
for the degree of Master of Science in Biochemistry

Department of Biochemistry, Microbiology and Immunology
Faculty of Medicine
University of Ottawa

Your file Votre référence
ISBN: 0-612-90072-X
Our file Notre référence
ISBN: 0-612-90072-X

ABSTRACT

Mitochondria in all cell types undergo frequent fission and fusion events, and these dynamics determine the overall morphology of the organelle in cells. Two important GTPases have been recently identified that regulate mitochondrial membrane activity, a dynamin related protein (DRP1) required for fission, and the novel fusion GTPase, Mitofusin2. Mitofusin2 is an outer mitochondrial membrane protein and, like other GTPases involved in membrane fusion events, the N-terminal GTPase domain is exposed to the cytosol, such that it could interact with and recruit potential cytosolic proteins. The work documented in this thesis aims towards understanding the specific role of this unique GTPase in regulating mitochondrial fusion events, and to identify potential interacting proteins that work together with Mfn2 to carry out this complex biochemical event. Two independent approaches were taken to identify interacting proteins, both a yeast two-hybrid screen and affinity chromatography using recombinant bacterial expressed Mfn2 protein as bait. The results of the affinity column suggest that Mfn2 was responsible for forming a stable multiprotein complex in the mitochondrial outer membrane. This study has also investigated the functional role of Mitofusin2 GTPase in the regulation and activation of mitochondrial fusion in mammalian cells and has uncovered a novel function for Mfn2 in stimulating mitochondrial fusion with complete matrix content mixing, and this activity is absolutely dependent upon the GTPase binding domain. The creation of a dominant active form of Mfn2 resulted in highly stimulated fusion and loss of the discreet Mfn2 puncta, suggesting Mfn2 is a regulatory GTPase that, upon GTP binding, is capable of signalling fusion events to wild type mitochondria. The

fused mitochondrial reticulum also showed increased protection against free radical damage, demonstrating a novel physiological function for mitochondrial fusion in cellular protection. This work presents the first data describing the nucleotide binding properties of Mfn2 and a novel function is identified for the Mfn2 GTPase activity in the synchronization and stimulation of mitochondrial fusion.

ACKNOWLEDGMENTS

I would first like to thank Dr. Heidi McBride for giving me an opportunity to pursue this degree under her supervision. I am grateful for her constant support, kindness, friendship and lot of encouragement.

I would like to thank Dr. Zemin Yao and Dr. Mary Ellen Harper, members of my thesis Advisory Committee, for their advice and suggestions. Special thanks go to Dr.Mary-Ellen Harper for her time and patience spent in reviewing my thesis.

I would like to thank our lab technician, Mr. Rodolfo Zunino, for doing the nucleotide binding assays. (Section 3.2(b), Figure 15)

I would like to thank Margaret Nelson in our lab for performing the PEG fusion assay. (Section 3.2(e), Figure 18)

I would like to thank Peter Rippstein for helping us with the Electron Microscopy. (Section 3.2(f), Figure 19)

I would also like to thank all the members of our lab for their friendship.

I am very grateful to my family for their constant support, affection and patience.

I am forever indebted to my mother Smt. Gangaraju Rajeswari for her understanding, endless patience and encouragement and whose presence made the completion of my graduate work possible.

Words cannot truly express my deepest gratitude to my loving husband, Jawahar B Baskar for his invaluable support, patience and understanding.

Last but not the least, I would like to thank my daughter, Nandita R Jawahar for her tons of love and understanding – she allowed me spend most of my time on this thesis.

Dedication

This thesis is dedicated to my father Late Sri Gangaraju Sivarama Raju, who is my inspiration and whom I love the most.

Abbreviations

β-ME = β-mercapto ethanol

CFP = Cyan fluorescent protein

Drp1 = Dynamin related protein 1

Fzo1p = Fuzzy onion 1 protein

GAP = GTPase activating protein

GDP = Guanosine di phosphate

GEF = Guanine exchange factor

GTP = Guanosine tri phosphate

GTPase = Guanosine triphosphatase

His = Histidine

HRP = horse radish peroxidase

Leu = Leucine

Mant-GDP = 2'-(or –3')-O-(N-methylanthraniloyl) guanosine 5'-diphosphate

Mfn2 = Mitofusin 2

$\Delta\Psi$ = mitochondrial electrochemical potential

MtDNA = mitochondrial DNA

ONPG = O-nitrophenyl β-D-galactoside

PBS = Phosphate buffer saline

P-Loop = phosphate binding loop

PEG = Polyethylene glycol

SDS-PAGE = sodium dodecyl sulphate-Polyacrylamide gel electrophoresis

TMRE = tetramethylrhodamine ester

Trp = Tryptophan

μl = microlitre

YFP = yellow fluorescent protein

YPD = Yeast extract, peptone and dextrose

TABLE OF CONTENTS

LIST OF TABLES

LIST OF FIGURES

1. Introduction

1.1 History of mitochondrial dynamics:

The mitochondria are very important organelles playing essential roles in a variety of biochemical pathways including ATP production, amino acid synthesis, steroidogenesis, maintenance of calcium homeostasis, and the initiation of programmed cell death (Ranger et al., 2001; Saraste, 1999; Stocco, 2001; Wallace, 1999). In textbooks, mitochondria are commonly depicted as static, oblong shaped structures scattered throughout the cytoplasm. Recent work has changed our old images of this ancient, double membrane organelle and they have become the centre of the fascinating new field of mitochondrial dynamics. Now we understand that, in living cells, mitochondria often form tubular networks with an ability to change size and shape which takes place due to frequent fission and fusion events (Bereiter-Hahn and Voth, 1994). The need for mitochondrial fission was obvious because mitochondria are not created de novo, and the mitochondrial segregation to dividing cells absolutely requires the fission of mitochondria before or during cell division. The concept that mitochondria fuse became evident in an adult cell when an experiment was performed that visualized mitochondrial dynamics following cell fusion by fluorescence microscopy. The mitochondrial DNA from one cell was found in nearly all mitochondria lacking DNA of the second cell almost immediately following cell fusion (Hayashi et al., 1994).

All of these aspects of mitochondrial dynamics were observational and controversial and the molecular details came slowly using a number of approaches. The first molecules identified as playing essential roles in the maintenance of mitochondrial morphology were the mitochondrial kinesins, KIF1B and KIF5 (Nangaku et al., 1994; Tanaka et al., 1998). These, along with mitochondrial dyneins are essential for

mitochondrial motility along microtubules in mammalian cells (Schroer et al., 1989). In addition to motility factors, mutagenesis studies in the yeast *Saccharomyces cerevisciae* have identified numerous proteins required for the maintenance of proper mitochondrial morphology. These genetic screens searched for mutations in proteins that led to yeast cells deficient in segregating mitochondria into the buds, as well as deficiencies in mtDNA segregation into dividing mitochondria. Screens performed by the laboratories of Robert Jensen, Michael Yaffe, Lisa Pon, Janet Shaw and Benedikt Westermann were able to assign these proteins into a number of different functional classes. Some proteins were important in maintaining housekeeping functions, like assembly of the cytoskeleton (Boldogh et al., 1998; Simon et al., 1997), and others were more directly involved in mitochondrial fission and fusion (members of the dynamin family of proteins, and other novel GTPases (Bleazard et al., 1999; Otsuga et al., 1998; Sesaki and Jensen, 1999)). By 1998 there were a number of proteins suggested to be involved in mitochondrial shape and dynamics, which are collected in a review (Hermann and Shaw, 1998a). These proteins are now the basis for much of today's research into the subject of mitochondrial dynamics.

Although some of the proteins identified in these screens do not have obvious orthologues in higher eukaryotes, at least two of the candidates, designated Fuzzy onion protein (Fzo1p) and Dynamin-related protein (Drp1), are clearly conserved. Together, they are now considered part of the core machinery for maintaining mitochondrial distribution and morphology. More recent studies in yeast also demonstrated that mitochondria are much more active than we thought since they fuse and /or divide once every 2 minutes on average (Griparic and van der Bliek, 2001; Yaffe, 1999). Importantly,

the definitive evidence demonstrating the occurrence of mitochondrial fusion in mammalian cells came in August 2001. Mitochondrial geneticists, Hayashi and colleagues created two lines of transgenic mice, each with distinct mutations, crossed them and demonstrated that the mitochondria in all cell types examined had intermixed their matrix compartments, which rescued the diseased phenotypes (Nakada et al., 2001). The group also published a similar paper demonstrating mitochondrial DNA complementation in human cultured cells (Ono et al., 2001). Therefore, although there has been controversy in the past concerning the extent of mitochondrial dynamics in mammalian cells (Enriquez et al., 2000; Takai et al., 1999), today it is clear that this is an important aspect of mitochondrial biology in all cells. But our understanding of the relationship between mitochondrial morphology and function is extremely limited and, hence, it is important to investigate the basic principles and mechanisms that govern mitochondrial dynamics in mammalian cells.

1.2 Physiological roles of mitochondrial dynamics

Using the knowledge gained from mechanistic studies of mitochondrial dynamics and developing more tools, it will be easier to test the physiological roles of fusion and fission in mitochondria. At the moment, some of the ideas as to why mitochondria fuse and divide are as follows.

1.2 (a) Mitochondrial DNA segregation/maintenance:

The physiological importance of mitochondrial fusion is not very clear because there is no obvious cargo to be transported or exchanged between the mitochondria. Hayashi and colleagues propose that mitochondrial DNA (the number of mitochondrial

DNA per mitochondrion ranges between 10 and 100 copies) might be one of the cargoes that is to be exchanged between mitochondria. According to this model, mitochondria function as a unified reticulum and fusion between mitochondria with distinct mutations in their mitochondrial DNA will rescue each other and buffer individual mtDNA mutations (Nakada et al., 2001; Ono et al., 2001). They hypothesize that this would increase the time it may take for mutant mitochondrial DNAs to become dominant over the wildtype and produce a disease phenotype. Interestingly, there is a wide variation in the phenotypes observed in different patients that carry the same mitochondrial mutations, which presents the possibility that, in some cases, the disease symptoms may be enhanced due to insufficient intermixing of their mitochondria.

A study by Ronald A.Butow and colleagues suggest that there is an active mechanism that segregates the transmission of mitochondrial DNA into the bud and that sorting accompanies a continuous and direct transfer of mitochondria to the bud (Okamoto et al., 1998). However it remains unclear how the mutated mtDNA could signal to the regulatory proteins to trigger or stimulate fusion.

1.2 (b) Apoptosis:

Initiation of apoptosis is another potentially important function of mitochondrial dynamics. The vital function of the mitochondria in the initiation and progression through cell death has been the subject of intense research over many years (Desagher and Martinou, 2000; Ranger et al., 2001; Zamzami and Kroemer, 2001). An important study by Richard Youle and colleagues (Frank et al., 2001) provides data that links mitochondrial fission/division with programmed cell death. They demonstrated that mitochondrial fission is blocked in cells transfected with dominant negative

mitochondrial dynamin (DRP K38A) and that apoptosis was arrested at a stage prior to cytochrome c release. The authors of this paper conclude that mitochondrial fission is essential for cytochrome c release though the reason for this is not clear. Another recent study by Richard J.Youle and colleagues demonstrated that Drp1 that plays a role in mitochondrial fission and Mfn2, which is responsible for mitochondrial fusion, colocalizes with Bax which is a proapoptotic member of the Bcl-2 family (Karbowski et al., 2002). From all these observations, it is clear that mitochondrial fission is an essential aspect of programmed cell death and it can then be predicted that Fzo1p/Mfn2 may be inactivated for cell death to occur.

1.2 (c) Energetics/Metabolism:

Mitochondria are well known for playing essential roles in energy production and metabolism but so far there has been no direct relationship between morphology and function. However, there is some indirect evidence suggesting the relation between the two. First, a recent study by Gary Ruvkun and colleagues on C.elegans longevity suggests that the genes, which are essential for mitochondrial function, have very important roles in determining the lifespan of C.elegans. This study identified a mutation in a mitochondrial gene that impairs mitochondrial function and is associated with longer life spans of C.elegans. These worms had fragmented and distorted mitochondria and had lower levels of ATP, lower oxygen consumption but had increased resistance to free radicals suggesting that a link between normal electron transport is necessary for both mitochondrial function and normal fission/fusion (Lee et al., 2003). Second, a recent study by Manuel Rojo and colleagues suggests that an inner membrane potential is required for mitochondrial fusion in human cells. When membrane potential is

uncoupled, fragmentation results which means Drp is recruited but it is not yet clear whether activity of Mfn2 has been altered as well (Karbowski et al., 2002). Regardless of the mechanism, this suggests that changes in the respiratory state may trigger morphological changes.

1.3 Mechanism of mitochondrial fusion and different methods considered for studying the process.

In order to understand the aspects of mitochondrial fusion, it is important to consider the complexity of the fusion event. Mitochondria, being double membrane organelles, are faced with a challenge of fusing four membranes, which requires a number of distinct events, which must be spatially and temporally regulated. First, mitochondria have to move towards each other along microtubules and actin cables, which require proteins of the kinesin and dynein family (Nangaku et al., 1994; Schroer et al., 1989; Tanaka et al., 1998). It remains unclear how the recruitment of these motor proteins to the mitochondrial surface is regulated according to the needs of the cell. Second, it is assumed that there is some regulatory and tethering machinery that allows two independent mitochondria to dock together. Once the two mitochondria have become tethered, their membranes need to become closely apposed in order to engage a pore through which bilayer mixing can occur, as illustrated in Figure 1. The assembly of such a pore could involve proteins such as the coiled coil containing viral fusion proteins or SNAREs that function in vesicular transport (Mayer and Wickner, 1997; Rothman and Warren, 1994). Finally, once the outer membrane bilayer has mixed, the inner membranes must also recognize each other and form a fusion pore in order for full matrix content mixing.

Figure1: Model for membrane fusion:
1. Recruitment of proteins of the fusion machinery docks the outer membranes of two mitochondria.
2. The sites where the mitochondria are docked or tethered. Tethering could trigger the rearrangement of proteins in the outer membrane in order to allow the assembly of a pore. (red and green becomes yellow).
3. Similarly, the inner membrane bilayers also fuse to allow matrix content mixing. Presumably the initial event is also a tethering reaction mediated by specific fusion machinery.
4. Bilayer fusion requires the assembly of a pore to facilitate lipid mixing resulting in the fusion of the two membranes (shown in yellow).

1. Signals to fuse

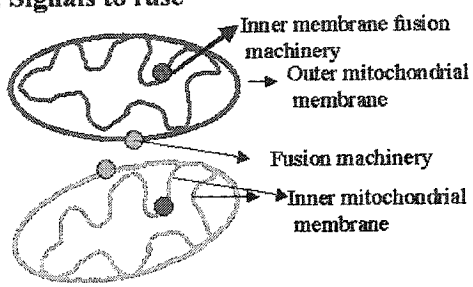

2. Selection of docking sites(tethering)

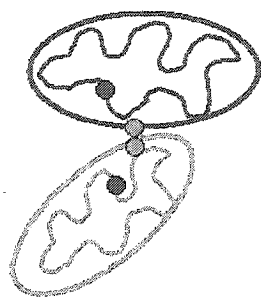

3. Outer membrane fusion followed by fusion of inner membranes.

4. Bilayer fusion

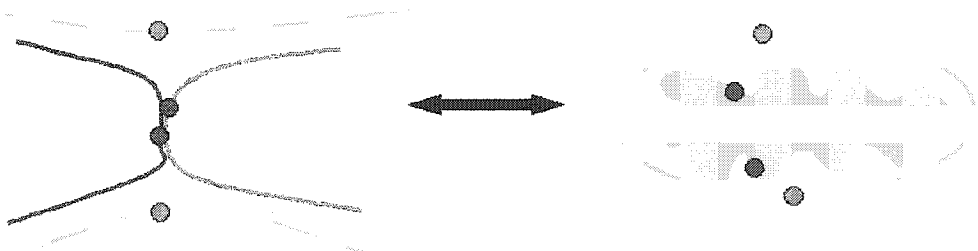

For each of these steps, studies in other membrane fusion events have demonstrated that a complex network of protein interactions are involved which coordinate these events in a temporospatial manner to make sure the specificity of fusion events within the cell (Zerial and McBride, 2001). The mitochondrial outer membrane GTPase, Fuzzy onion (Fzo1p) of yeast *Saccharomyces cerevisciae* and *Drosophila melanogaster* was first identified to play an essential role in mitochondrial fusion (Hales and Fuller, 1997; Hermann et al., 1998b). When fusion is blocked in yeast cells lacking Fzo1p, mitochondrial fission continues and the phenotype observed is of fragmented mitochondria that ultimately lose their ability to segregate mtDNA (Hermann et al., 1998b; Rapaport et al., 1998; Sesaki and Jensen, 1999). When the Drosophila Fzo1p gene was deleted, the mitochondria in the sperm tail were packed together but not fused and looked like an onion by EM section. This resulted in a sterile male phenotype since the sperm couldn't swim (Hales and Fuller, 1997). Drosophila and human genomes contain at least 2 isoforms of Fzo1p (Hwa et al., 2002; Santel and Fuller, 2001), and the human isoforms are encoded by separate genes, Mitofusin1 (Mfn1) and Mitofusin2,(Mfn2)(Santel and Fuller, 2001). The alignment of Mitofusin 1 and Mitofusin 2 with the orthologues in yeast and Drosophila is shown in Figure 2. The reason for the gene duplication of Fzo1 in higher organisms remains unknown, however Mfn1 and Mfn2 are ~60% identical and ubiquitously expressed. The protein spans the outer bilayer twice, with both termini facing the cytosol (Rojo et al., 2002) as shown in Figure 3(a) and the schematic diagram of the domain organization of Fzo1p is shown in Figure 3(b). In yeast, Fzo1p protein has at least 10 amino acids exposed to the intermembrane space, however in mammalian Mfn1 and Mfn2, this region has been reduced to 2 residues.

Figure 2: Fzo/Mfn alignment:
Shown in red are the domains in the phosphate-binding region, blue boxes represent the predicted trransmembrane domains and the regions underlined with green are the predicted coils. Human Mfn1 and Mfn2 are 60% identical to each other and Drosophila Fzo1p is 27.5% identical to human Mfn2 and S.cerevisiae Fzo1p is 11.2% identical to Mfn2.

Fzo/mitofusin alignment

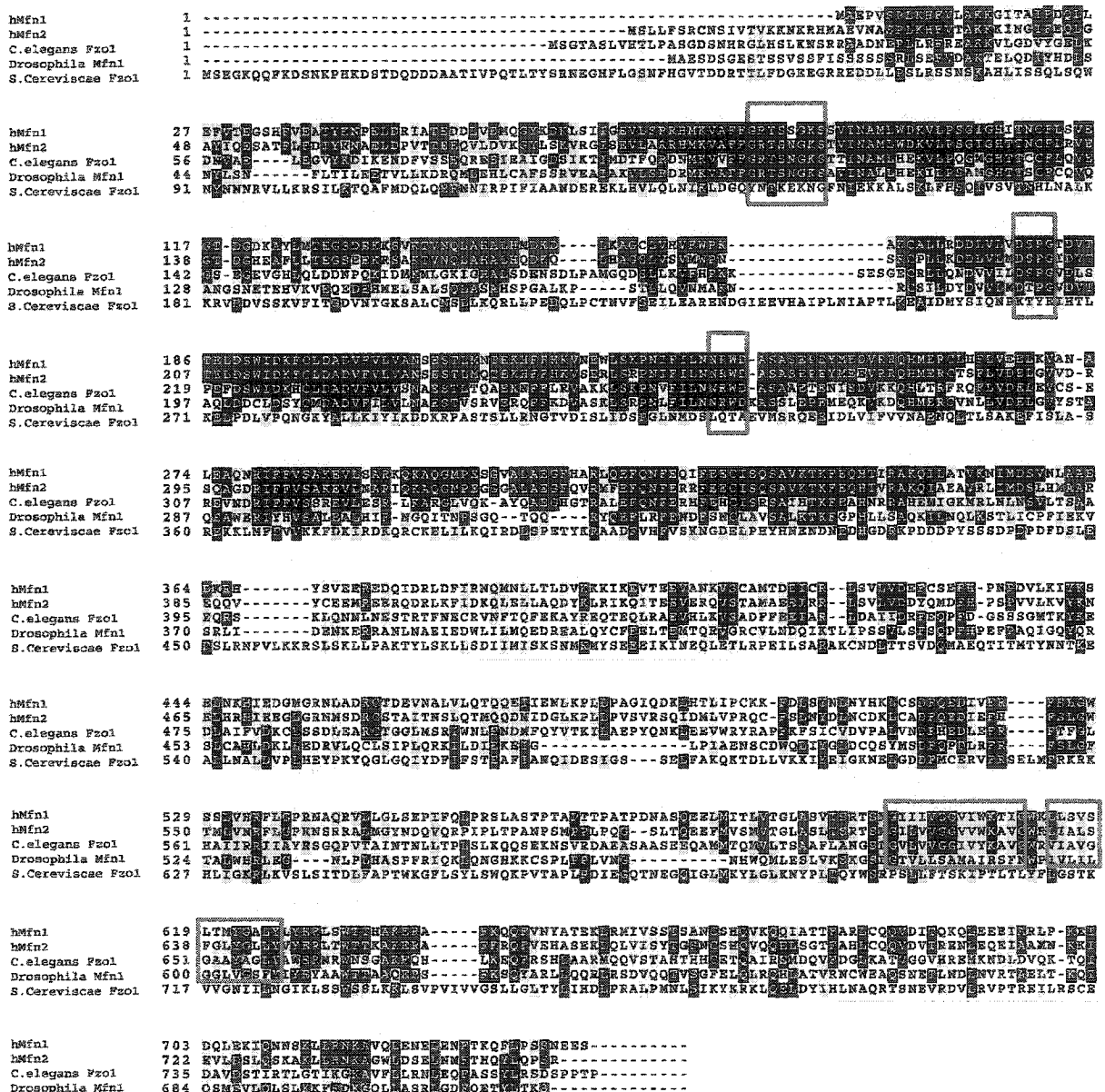

Figure 3: Orientation and schematic diagram of domain organization of Fzo1p/Mfn2

(a): Orientation of Fzo1p/Mfn2 in the outer mitochondrial membrane: This figure illustrates the orientation of Fzo1p/Mfn2 on the outer membrane of the mitochondria. It spans twice in the outer bilayer with the GTPase domain and coils exposed to the cytosol

(b): **Schematic diagram of domain organization of Mfn2:** Shows the domain organization of Mfn2 where it has the GTP binding motifs, two coiled coil regions and TMD which stands for transmembrane domains (a transmembrane domain consists of stretches of 15-30 predominantly hydrophobic residues).

(A)

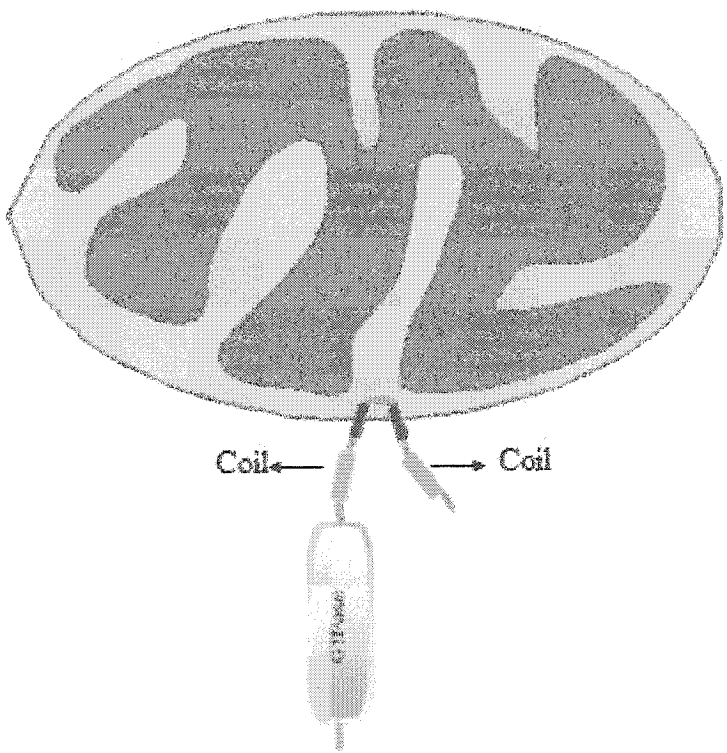

(B)

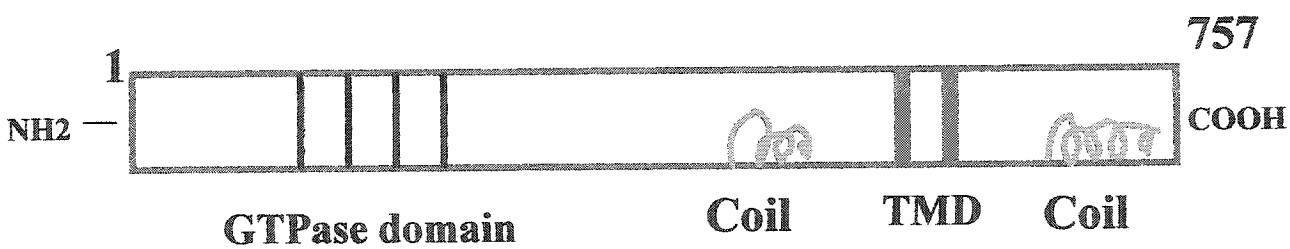

Data from yeast suggests that this intermembrane space region is important for the formation of contact sites between the outer and inner membranes, and the loss of these sites compromised the function of Fzo1p (Fritz et al., 2001). Since the GTPase domain is exposed to the cytosol, it could act as a key player in the recruitment of cytosolic effector proteins. The cytosolic carboxy terminal region is predicted to form a coiled coil, highly reminiscent of the SNARE proteins, which are absolutely essential for all vesicular fusion events in the cell. Looking only at the predicted secondary structure of Mitofusin2, it is tempting to envision that the mitochondria have evolved a single protein, which incorporates the regulatory function of the Rab GTPases (Novick and Zerial, 1997) and the coiled coils of the SNAREs (Weber et al., 1998) to drive bilayer fusion directly. However Mitofusin2 is a novel GTPase and it's important to understand how this protein is going to function in mitochondrial fusion. Since, the common thread in all GTPases is that the switch regulates protein interactions, my first objective was to identify the interacting proteins of Mfn2. Three different methods were considered namely, yeast two-hybrid screen, affinity chromatography and co-immunoprecipitation. Each method is important and has its own advantages and disadvantages, as described below.

1.3(a) Identifying interacting proteins: a comparison of methodology

General considerations: The two-hybrid system offers some advantages over other biochemical methods for detecting interactions between proteins, such as immunoprecipitation and affinity chromatography (Bartel et al., 1993; Chien et al., 1991). The most significant advantage is that two-hybrid systems require neither purified proteins nor antibodies which can be very rate limiting with a new project like this. The methodology is used to screen entire libraries of genes for interactions against an

individual protein, but in addition, pairs of known proteins can be tested against each other for possible interactions and also groups of proteins can be tested in pair wise combinations. Another advantage of two hybrid systems is that the experiments are conducted in living eukaryotic cells, hence the proteins are more likely to be in their native state than proteins expressed in bacteria as in the biochemical methods.

Access to total proteins: In yeast two hybrid systems, the interaction between the bait and target takes place in the nucleus of yeast and hence only soluble proteins can be pulled out from the screen. An additional disadvantage of two hybrid screens is that they are totally based on the library which is limited by the activity of reverse transcriptase because only one out of six fused DNAs is in the correct frame, thereby increasing the total number of independent clones to be screened to over a million. In order to avoid missing the interactions that take place with the proteins on the membrane, biochemical approaches were also considered where both membrane proteins and soluble proteins are applied to the column, thereby allowing all possible interactions to occur.

Stringency of interactions: Two hybrid systems are quite sensitive in that they can detect even transient interacting proteins, often missed by methods like affinity chromatography and immunoprecipitations. However with high sensitivity, weak and non-specific interactions can also lead to false positives (Serebriiskii et al., 2000). The main disadvantage of two-hybrid screens is a high incidence of false positives and so the requirement for biochemical evidence to support the interaction is essential. In contrast, affinity chromatography and co-immunoprecipitations include stringent washes and incubations thereby increasing the chances that only stable and specific interactions are identified.

Mass Spectrometry limitations: In two hybrid screens, the gene sequences for the interacting proteins are contained in the clones that score positively, facilitating the retrieval of genes of interest. In affinity columns, the bands from the gel are subjected to mass spectrometry. Data base searches have to be done in order to identify the proteins and once the proteins are identified, the cDNA must be obtained. All of these steps along with outside collaborations make the biochemical procedure a bit time consuming.

With full knowledge of the advantages and disadvantages of the two-hybrid and affinity chromatography approaches, it was decided to take a complimentary approach and attempt both techniques for identifying interacting proteins of Mfn2. Co-immunoprecipitaation experiments clearly require specific antibodies raised against Mfn2, which were not yet available during this study. Part of my project was also to prepare recombinant protein in order to inject rabbits for the purpose of generating Mfn2 specific antibodies; however this work remains incomplete and is not presented within this thesis.

1.3 (b) Dissect the role of Mfn2 in mitochondrial fusion

GTP cycle: Mechanisms of a molecular switch: Mitofusin contains a clear, but unique GTPase binding domain; therefore the second objective of my project was to consider the mechanism of GTPase action in known classes of GTPases in order to understand the possible role of Mitofusin 2 in mitochondria fusion. It is possible that the Mitofusin2 could behave like a regulatory GTPase (example Rab proteins) where the nucleotide cycle is tightly regulated by exchange factors (GEFs) and GTP activating proteins (GAPs) as shown in Figure 4(a). Once in the GTP bound form, each Rab recruits a subset of effector proteins responsible for performing downstream functions (Zerial and

McBride, 2001). For regulatory GTPases, the affinity for nucleotide is very high (~10^{-7} μM) and the rates of GTP hydrolysis and the exchange of nucleotide are usually slow (the intrinsic GTP hydrolysis rate is ~10^{-4}/second). Another possibility is that Mfn2 could act like dynamin family of GTPases (mechanoenzymatic GTPases), which have a much lower affinity for nucleotide (0.5-2.5 μM) and the intrinsic rates of hydrolysis are extremely high (the intrinsic GTP hydrolysis rate is ~2-5/second) since the GTPase activating protein (GAP) is encoded in the same polypeptide (Danino and Hinshaw, 2001; Song and Schmid, 2003). One more possibility is that the GTPase activity of Mfn 2 might be involved in a conformational change within a multiprotein complex like SRP (Signal Recognition Particle) or EFTu (Elongation factor-Tu) complex which have a lower affinity for nucleotide (1-2μM) (Vetter and Wittinghofer, 2001; Jagath et al., 1998). Such striking differences in nucleotide activity between the Rab family of regulatory GTPases, Dynamin families and SRP or EFTu complexes have profound implications for their functional mechanisms. Generally the function of GTPase activity in regulatory GTPases is to signal the recruitment of downstream effectors. Dynamins, on the other hand function mechanically to exert force (Figure 4(b)) where as the function of the GTPase activity in SRP or EFTU complexes is to induce a conformational change within a multiprotein complex in order to alter the affinity to specific substrates (Figure 4(c)).

Creation of a dominant active form of Mfn2: Studies overexpressing either isoform (Mfn1 or Mfn2) within cultured cells has been shown to cause a mitochondrial clustering phenotype (Rojo et al., 2002; Santel and Fuller, 2001). Importantly, experiments over expressing Mfn2 harbouring a mutation of the conserved lysine of the

Figure 4: General mechanism of action of different GTPases

(a): General mechanism of action of regulatory GTPases where the nucleotide state is regulated by GEFs and GAPs and work is performed by effector proteins. GBP stands for GDP binding protein.

(b): General mechanism of action of mechanoenzymatic GTPases where the nucleotide hydrolysis causes a conformational change that generates force to drive the work. For example membrane fission.

(c): General mechanism of action of GTPases where a conformational change induces binding to the substrate

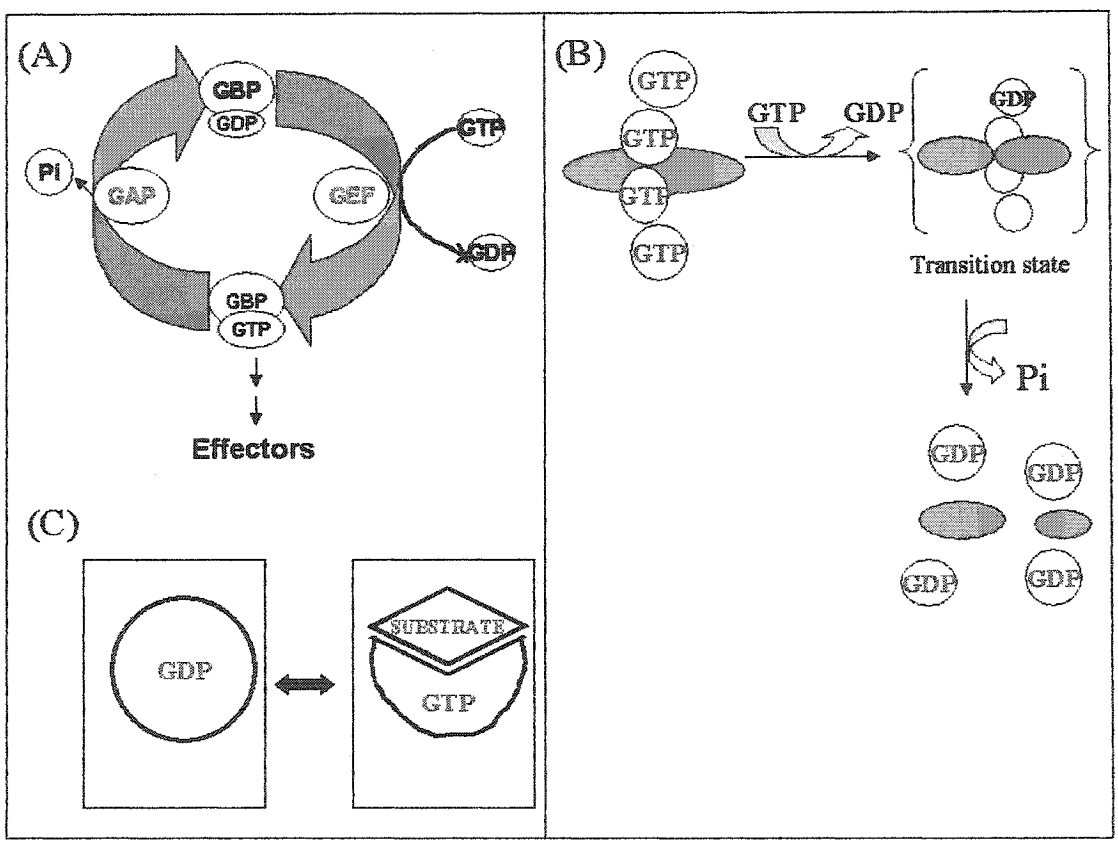
(A)
GBP
GDP
GTP
GDP
Pi
GAP
GEF
GBP
GTP
Effectors
(B)
GTP
GTP
GTP
GTP
GTP
GDP
GDP
Transition state
Pi
GDP
GDP
GDP
GDP
(C)
GDP
SUBSTRATE
GTP

phosphate-binding loop ($Mfn2_{K109T}$), demonstrated a role for nucleotide binding in the development of the fused DRP1K38A mitochondrial phenotype (Labrousse et al., 1999; Santel and Fuller, 2001; Smirnova et al., 2001). These results confirmed that the function of Mfn2 requires its GTPase activity, however the experiments did not identify the precise function for the GTP switch mechanism. One possibility highlights the increased complexity of mitochondrial fusion due to the fact that the mitochondria have two membrane structures that must both fuse for matrix content mixing to be completed. It is not yet known whether the outer and inner membrane fusion events are directly coupled, or if they fuse using completely independent machineries Of course these potential functions for Mfn2 are not mutually exclusive (and do not exclude other possible functions) but illustrate a number of events likely to be regulated by a GTPase switch. The experimental approach designed in order to identify a more precise function for Mfn2 was to generate a mutation that maintains the ability to bind nucleotide, but whose nucleotide activity (rates of exchange and/or hydrolysis) is altered. In order to distinguish the function of the switch mechanism, it is essential that mutations can be made that stabilize the GTPase in either the "on", GTP bound form or the "off" GDP bound form. The difficult question was how to determine which specific amino acid mutations should be made in order to alter the nucleotide state of a completely novel GTPase family member. This is generally done by first comparing the intrinsic rates of nucleotide exchange and hydrolysis of the purified recombinant protein to known GTPases, like those in the Ras or Dynamin families. Unfortunately, the predicted soluble GTPase domain of Mfn2 is completely insoluble when expressed alone, and there has been no report of nucleotide affinities or intrinsic rates of hydrolysis for Mfn2. However, in the

analysis of the crystal structure of GTP bound guanylate binding protein (GBP1), it was suggested that the guanidinyl group of an arginine residue within the P-Loop may contribute to the nucleophilic attack by water on the tertiary phosphate of GTP to stimulate hydrolysis (Prakash et al., 2000). This chemistry would be mechanistically equivalent to the GTPase activating proteins (GAPs), many of which introduce an arginine finger into the nucleotide binding pocket to trigger hydrolysis (Albert et al., 1999; Mandiyan et al., 1999; Rak et al., 2000; Resat et al., 2001; Rittinger et al., 1997). If this line of thinking is extended, any observed arginine within the P-Loop of a nucleotide-binding consensus may indicate that the intrinsic rate of hydrolysis is high. Interestingly, when the residues within the P-Loop of Mfn2 were analyzed, there was a conserved arginine present in both isoforms of Fzo/Mfn from drosophila, C.elegans and humans. Interestingly, the *P-Loop* of higher organisms was completely divergent from that in yeast Fzo1p, suggesting that the intrinsic rates of exchange and hydrolysis may have evolved new physical properties in higher organisms. Therefore, since the primary sequence of human Mfn2 contains an arginine within the phosphate binding loop (P-Loop), the entire variable region of the P-Loop was mutagenized to mimic the small, hydrophobic residues of the activated form of Ras (RasG12V)(Futatsugi and Tsuda, 2001; Tong et al., 1989) in an effort to retain the nucleotide binding consensus GxxxxGKS, but to alter the intrinsic GTPase properties in order to keep it bound to GTP (Figure 5). Through the manipulation of the GTP binding site of Mfn2, experiments were designed in order to examine the consequences of the GTPase switch in mitochondrial fusion events. This work is presented in Section 3.2 "Dissection of role of Mfn2" and represents the major contribution to knowledge contained within this thesis.

Figure 5: Variable residues of P-loop of the Fzo1p orthologues
Sequences of the conserved P-Loop of the Fzo1p orthologues are compared with Ras. The star indicates the position of the RasG12V mutation, circles indicate residues identified within the Ras crystal structure that interact with the nucleotide and the square indicates the residue interacting with the co-ordinating magnesium ion (Krengel et al., 1990; Vetter and Wittinghofer, 2001).

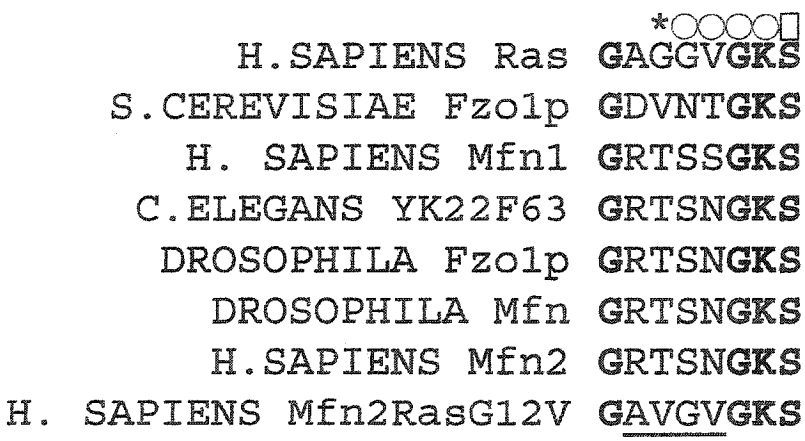
*○○○○□
H.SAPIENS Ras GAGGVGKS
S.CEREVISIAE Fzo1p GDVNTGKS
H. SAPIENS Mfn1 GRTSSGKS
C.ELEGANS YK22F63 GRTSNGKS
DROSOPHILA Fzo1p GRTSNGKS
DROSOPHILA Mfn GRTSNGKS
H.SAPIENS Mfn2 GRTSNGKS
H. SAPIENS Mfn2RasG12V GAVGVGKS

1.4 Objectives

The objectives of this thesis are to understand the role of Mfn2 in the mechanism of mitochondrial fusion by taking two approaches namely

1. To identify the interacting proteins of Mfn2 that work together with Mfn2 to carry out the complex biochemical event of fusion by performing a yeast two-hybrid screen and affinity column

2. To dissect the function of Mfn2 by

(a) Generating mutants and performing morphological assays by over expressing the wild type and mutants

(b) Performing GTP binding assays to understand the nucleotide binding activity

(c) Performing assays to investigate the physiological function for mitochondrial fusion.

2. Materials and Methods

2.1 Identification of interacting proteins:

In order to identify the interacting proteins of Mfn2, a yeast two-hybrid screen was performed using the predicted soluble GTPase domain of Mfn2, which is Mfn2 (1-560).

2.1 (a) Yeast two hybrid screen: Principle

The yeast two-hybrid system is based on the interaction of proteins synthesized by two hybrid genes made in two separate but compatible yeast vectors [Bartel et al., 1993; Chien et al., 1991]. The vectors are transformed and maintained within yeast strain with appropriate auxotrophic mutations. One of the hybrid genes is made by fusion between DNA binding domain of a transcription factor (pLexA vector) and the bait, which is Mfn2 (1-560). The other hybrid gene is the fusion between the activation domain of a transcription factor (pGAD vector) and a test protein, which is HeLa library. Plasmids encoding these fusions are introduced together into a yeast strain that contains the reporter genes, which in our case are Histidine and β-galactosidase. The DNA binding fusion protein (pLexA-Mfn2 (1-560)) will recruit the protein products expressed from the library that are fused with the transcriptional activators which will allow transcription of reporter proteins. The gene encoding either the DNA-binding domain hybrid or activation domain hybrid is under the control of a yeast promoter, derived from the ADH1 (alcohol dehydrogenase) gene. The schematic representation of the principle is shown in Figure 6. The schematic diagram describing the methodology for yeast two-hybrid screen is shown in Figure 7.

Figure 6: Principle of a yeast two-hybrid assay:
The yeast two-hybrid system uses transcription of yeast reporter genes to measure the protein interaction. One of the two proteins (Mfn2) is expressed as a fusion to a DNA-binding domain (pLexA) from a transcription factor and the other (X) is expressed as a fusion to a transcription activation domain (pGADGH). If the fusion proteins interact, they activate transcription of specially designed reporter genes that carry binding sites for the DNA binding partner.

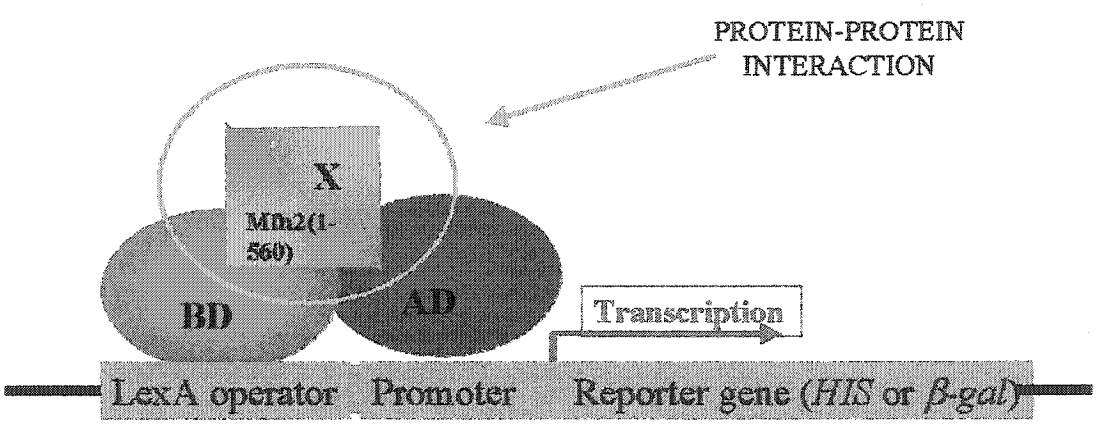

Reporter Protein

Figure 7: Schematic representation of the method for yeast two-hybrid screen:
This figure represents the different steps involved in the methodology of a yeast two-hybrid screen.

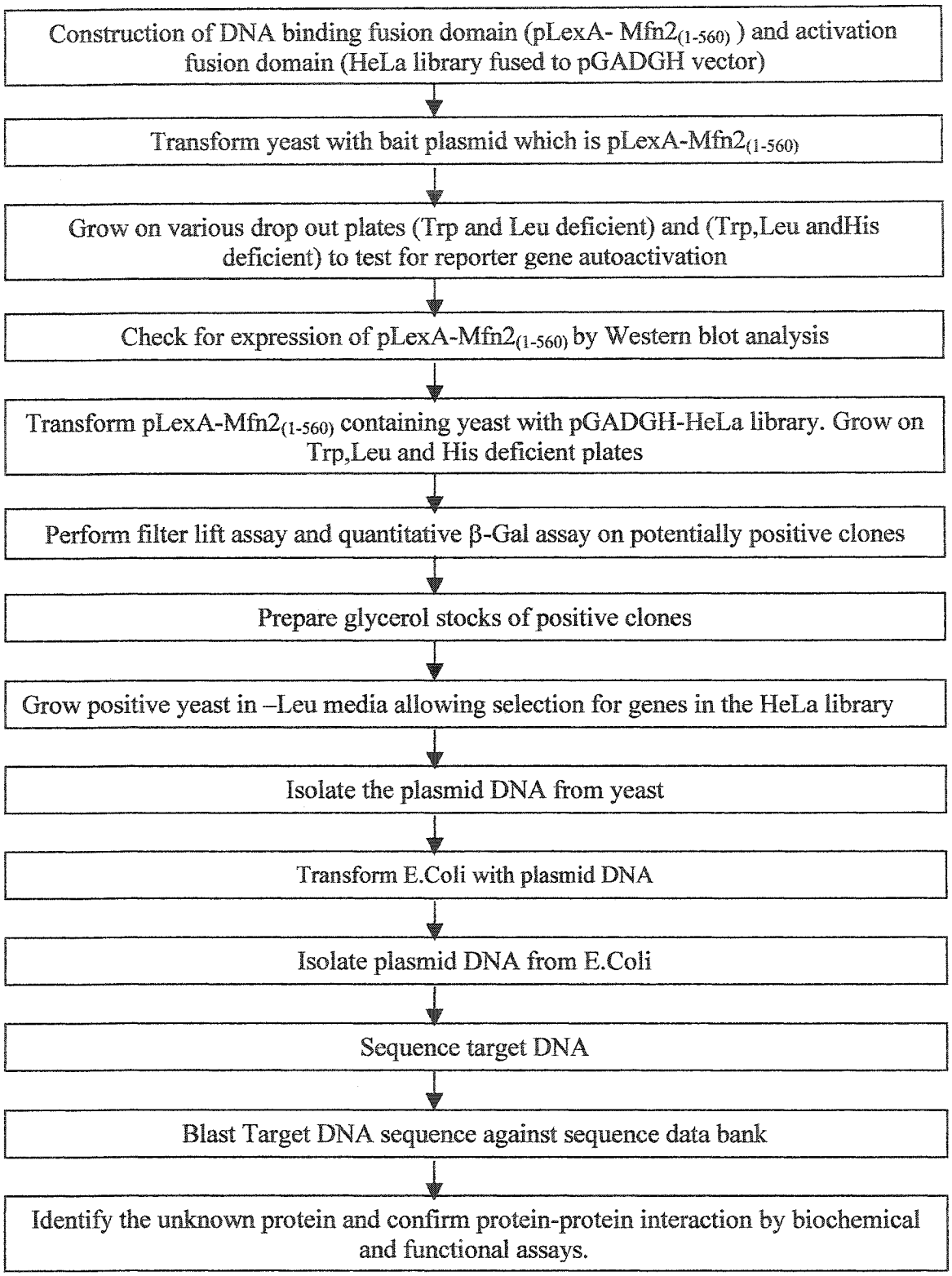
Construction of DNA binding fusion domain (pLexA- Mfn2(1-560)) and activation fusion domain (HeLa library fused to pGADGH vector)
Transform yeast with bait plasmid which is pLexA-Mfn2(1-560)
Grow on various drop out plates (Trp and Leu deficient) and (Trp,Leu andHis deficient) to test for reporter gene autoactivation
Check for expression of pLexA-Mfn2(1-560) by Western blot analysis
Transform pLexA-Mfn2(1-560) containing yeast with pGADGH-HeLa library. Grow on Trp,Leu and His deficient plates
Perform filter lift assay and quantitative β-Gal assay on potentially positive clones
Prepare glycerol stocks of positive clones
Grow positive yeast in –Leu media allowing selection for genes in the HeLa library
Isolate the plasmid DNA from yeast
Transform E.Coli with plasmid DNA
Isolate plasmid DNA from E.Coli
Sequence target DNA
Blast Target DNA sequence against sequence data bank
Identify the unknown protein and confirm protein-protein interaction by biochemical and functional assays.

(i) Preparation of construct

Kazusa DNA Research Institute, Japan, graciously provided the cDNA encoding human Mfn2 (KIAA0214). The cDNA encoding the predicted GTPase region of Mfn2 (Mfn2 (1-560)) was PCR amplified (Cloned Pfu polymerase, Stratagene) using primers appended with restriction enzymes EcoR1 and BamH1 for the sense primer and Xho1 and HindIII for the anti sense primer. This PCR amplified fragment was digested with Xho1 and EcoR1 and inserted for ligation into pLexA vector (gratefully obtained from Dr.Marino Zerial, Dresden, Germany) cut with Sal1 and EcoR1. pLexA-Mfn2(1-560) was then transformed in to the yeast. pLexA alone (negative control) and pLexA-Rab5Q79L (positive control) (gratefully obtained from Dr.Marino Zerial, EMBL, Heidelburg) were also transformed in to the yeast.

(ii) Yeast transformation

The YPD plates (regular growth media containing 1%yeast extract, 2% peptone and 2% glucose) were prepared by dissolving YPD agar media in water as per the manufacturer's instructions (Clontech, Palo Alto, CA). L40 yeast strain (gratefully obtained from Dr. Johnny Ngsee, Loeb Research Institute, Ottawa) was streaked on YPD agar plate and allowed to grow for 3 days at 30°C. The growth curve and doubling time of yeast was determined by growing 5 X 10^5 cells/ml yeast in liquid YPD media. The density of yeast was monitored using spectrophotometry by determining the absorbance of the culture at 600nm. A 25 µl yeast inoculum was isolated and resuspended in 1 ml of double distilled water. The cells were pelleted at 13,400g in a micro centrifuge for 5 sec and resuspended in 1 ml of 100 mM lithium acetate (Sigma, Oakville, ON) and incubated for 5 min at

30°C. The volume representing a single transformation reaction (250 µl) was placed in a separate micro centrifuge and the suspension was spun at 13,400g in a micro centrifuge for 5 sec and the supernatant was removed. The following components were added to the cell pellet, 240 µl of polyethylene glycol (50%W/V), 36 µl 1.0 M LiAc, 50 µl of 2mg/ml salmon sperm carrier DNA, 2 µg of pLexA-Mfn2 (1-560) and also 2µg each of pLexA and pLexA-Rab5Q79L, in separate reactions. The cell pellets were vortexed for at least 1 min to resuspend in the transformation mix and incubated at 42°C for 20 min, which allows the DNA to enter the cells. The cells were pelleted at 13,400g in a micro centrifuge for 10 sec and the supernatant was removed. The pellets were resuspended gently in 100 µl of double distilled water and the cell suspensions were plated onto tryptophan deficient plates (as mentioned below), which selects for the presence of pLexA-Mfn2 (1-560), pLexA and pLexA-Rab5Q79L and were allowed to grow for 3 days.

(iii) Yeast Growth

All the drop out plates were prepared by mixing Minimal SD Base and the appropriate drop out supplement as per the manufacturer's instructions (Clontech, Palo Alto, CA)

Tryptophan: Genes present on pLexA are responsible for the synthesis of tryptophan. Growth on SD agar plates lacking tryptophan reflects successful transformation of yeast with the bait.

Leucine: Genes present on pGADGH are responsible for the synthesis of leucine. Growth on SD agar plates lacking leucine reflects successful transformation of yeast with the library.

Reporters: Reporters include histidine and β-galactosidase. Synthesis of histidine is due to transactivation of (HIS) genes present in the L40 yeast strain. Growth on SD agar plates lacking histidine reflects that there is a protein-protein interaction between the bait and a library protein. Consequent β-galactosidase cleaves X-gal substrate to produce blue colour accounts for the LacZ expression. Intensity of blue colour reflects the strength of protein-protein interaction. To test for the reporter gene auto activation, the yeast with pLexA-Mfn2(1-560) was grown on various drop out plates (the growth should occur only on tryptophan deficient plates when there is no reportet gene autoactivation). Once it is found that there is no autoactivation, the expression of pLexA-Mfn2(1-560) is verified by a Western blot.

(iv)Western Blot to verify the expression of pLexA-Mfn2 (1-560) in yeast

It is important to check the expression of bait in the yeast by western blot analysis. In order to do this, the yeast cultures were prepared for protein extraction by Urea/SDS method. For this, a single colony of transformed yeast with bait, which is pLexA- Mfn2 (1-560), pLexA alone (negative control), and Rab5Q79L, which is a positive control, were inoculated in 2 ml of tryptophan deficient SD media and grown overnight at 30°C with shaking at 250 rpm. The overnight cultures were vortexed for 1 minute to disperse the cell clumps. For each of the overnight cultures, 2ml was diluted into 10ml of YPD media (1:5 dilution) and the cultures were incubated at 30°C with shaking until the OD at 600nm reached 0.4 - 0.6. The cultures were centrifuged at 1000 g (Sorvall RT 6000D centrifuge) for 5 minutes at 4°C. The supernatant was discarded and the cell pellet was

resuspended in 10 ml of ice-cold water. The pellet was recovered by centrifugation at 1000 g for 5 minutes at 4°C and frozen by placing the tube in liquid nitrogen. The cells were stored at -70°C until further use. The yeast cells were solubilised using prewarmed cracking buffer (8 M Urea, 5% w/v SDS, 40 mM Tris- HCl (pH6.8), 0.1 mM EDTA, 0.4 mg/ml Bromophenol blue, deionised water), containing a protease inhibitor mixture (0.1 mg/ml pepstatin A (Sigma,Oakville,ON), 0.03mM leupeptin (Sigma,Oakville,ON), 145 mM benzamidine (Sigma,Oakville,ON) and 0.37mg/ml aprotinin (Sigma,Oakville,ON)) and 50µl of 0.1M phenylmethyl-sulfonyl fluoride, (Sigma,Oakville,ON), heated at 70°C for 10 min followed by vigorous vortexing for 1 min. The unbroken cells and debris were pelleted in a micro centrifuge at 13,400 g for 5 min at 4°C and transferred the supernatants to fresh micro centrifuge tubes and placed on ice (first supernatants). The pellets were placed in a 100°C boiling water bath for 3-5 min and vortexed vigorously for 1 min. The unbroken cells and debris were pelleted in a micro centrifuge tube at 13,400 g for 5 min at 4°C and each supernatant was combined with the corresponding first supernatant. The samples were prepared in 2X sodium-dodecyl sulfate(SDS) sample loading buffer containing 1mM dithiotriol, boiled for 5 min at 90°C, and electrophoresed on a 10% polyacrylamide gel at 100V for 1.5 hours. The protein samples were transferred onto a nitrocellulose membrane at 70V for 2 hours. Non-specific protein binding to the membrane was blocked by incubating the membrane with PBS/0.1%W/V Tween/W/V 5% milk for 1hour shaking at room temperature. The membrane was probed with a mouse monoclonal anti-LexA antibody (Clontech, Palo Alto, CA) diluted 1:1000 in PBS/0.1%W/V Tween/5%W/V milk, for 1 hour at room temperature followed by washing 5 times in PBS/Tween for 5 minutes. The membrane was then probed with

secondary goat anti-mouse antibodies conjugated to horseradish peroxidase (HRP) (anti-mouse HRP) (Jackson Immuno research laboratories, Westgrove,PA) diluted 1:5000 in PBS/0.1% Tween/5% milk for 1 hour at room temperature. The membrane was then washed 5 times in PBS/Tween for 5 minutes and visualised using Chemiluminiscent substrate for detection of HRP (Biolynx INC, Brockville,Ontario) and developed using the Chemidoc system(University of Ottawa Heart Institute). Once the expression level of the bait in the yeast is known, the library is transformed into the yeast.

(v) Library transformation

In order to determine the scale up needed for the desired number of transformants with the library DNA, a 10X reaction (also tried a 1 X reaction to start with, but the efficiency was almost 0 colonies/μg library DNA and hence decided to go with a 10X reaction) was performed where the yeast strain containing the pLexA-Mfn2 (1-560) was inoculated into 25 ml of tryptophan deficient media and incubated at 30°C overnight which maintained pLexA-Mfn2 (1-560) during the growth phase. The next morning, the cells were grown into log phase in YPD media for only two doublings to avoid plasmid loss. The volume of cells that yielded 2.5 $x10^8$ cells for 50 ml of YPD culture was calculated and this volume was poured into an appropriate sterile centrifuge tube and the cells were pelleted at 3000 g for 5 min. The cell pellet was resuspended in 10 ml of pre-warmed (30°C) YPD and transferred to another sterile culture flask and incubated at 30°C while shaking at 200 g for 3 to 4 hrs until the cell titre reached 2 x 10^7 cells/ml. The cells were harvested by centrifugation at 3000 g for 5 min and the cell pellet was washed via resuspension with ½ volume of double distilled water and collected by centrifugation as above. The pellet was resuspended in 3 ml of 100mM sterile LiAc and transferred to

an appropriate centrifuge tube and incubated for 15 min at 30°C and the cells were pelleted again by centrifugation and the supernatant was removed. The components of the transformation mix (2.4 ml 50% PEG (Sigma, Oakville, ON), 360µl 1.0M LiAc, 500µl Salmon sperm DNA (2mg/ml)(Gibco BRL, Burlington, ON), 1 µg (0.5µl) HeLa library DNA) were added to the cell pellet and vortexed vigorously to resuspend the cell pellet and incubate at 30°C for 30 min and the heat shock was done at 42°C for 30min with mixing by inverting the tube for 15 sec after every couple of minutes. The cells were collected by centrifugation as above and the cell pellet was resuspended in 10 ml of double distilled water and plated on tryptophan and leucine deficient plates in duplicates in different dilutions of 1:100000, 1:10000 and 1:1000 in order to calculate the transformation efficiency and the rest was plated on tryptophan, leucine and histidine deficient plates (10 plates of 15cm each) and allowed to grow for 3-5 days at 30°C. The transformation efficiency was calculated/µg of HeLa library DNA and approximately $1x10^4$ colonies/µg of library DNA were screened. A 60 X scale was performed using 60µg of HeLa library in order to screen the full library, which consisted of 6 x 10^6 colonies. The interactions between pLexA-Mfn2 (1-560) and the genes in the library were checked by a colony lift filter assay.

(vi)Colony Lift Filter Assay

A qualitative colony lift filter assay was used to check the positive interactions (the interactions between the bait which is pLexA-Mfn2 (1-560) and the genes in the library). 300 colonies were grown on tryptophan, leucine and histidine deficient plates. For each plate of transformants to be assayed, a sterile VWR grade filter was presoaked

in a 2.5-5 ml of Z buffer/X-gal solution (Z buffer was prepared by mixing 0.06M Na_2HPO_4, 0.03M NaH_2PO_4, 0.01M KCl and 0.001M $MgSO_4$ and the pH was adjusted to 7.0; X-gal stock solution was prepared by dissolving 5-bromo-4-chloro-3-indolyl-β-D-galactopyranoside (Sigma, Oakville, ON) in N,N-dimethylformamide (DMF) at a concentration of 20 mg/ml(0.05 M); Z buffer/X-gal solution was prepared by mixing 100 ml Z buffer, 0.27 ml β-mercaptoethanol and 1.67 ml X-gal stock solution) and a clean dry filter was placed(by using forceps) over the surface of the plate of colonies to be assayed. Once the colonies clung to the filter, holes were poked through the filter into the agar in three or more asymmetric locations to orient the filter to the agar and when the filter was evenly wetted, the paper was carefully lifted off from the agar plate and transferred to a pool of liquid nitrogen for 10 sec. Once the filter paper was completely frozen, it was removed from liquid nitrogen and allowed to thaw at room temperature. The filter was carefully placed with the colony side up on the pre-soaked filter and incubated at 30°C and checked periodically for the appearance of blue colonies.

(vii) Quantitative β-Gal Liquid Assay

The interaction between the potential positives clones was tested quantitatively by performing quantitative β-Gal liquid assay. 5 ml overnight cultures of the clones (which turned blue in colour lift assay) in Tryptophan, Leucine and Histidine deficient media were prepared and 2 ml of the overnight cultures were transferred to 8 ml of YPD media. The fresh cultures were incubated at 30°C for 3-5 hr with shaking until the cells were in mid-log phase. 5 ml of cultures were placed into each of three 1.5 ml micro centrifuge tubes and centrifuged at 13,400g for 30 sec. The supernatants were removed and 1.5 ml

of Z buffer (as mentioned in the description of methods for the colony lift filter assay) was added to each tube, vortexed until cells were resuspended and the cells were centrifuged again at 13,400g. The supernatants were removed and each pellet was resuspended in 300 ml of Z buffer. 0.1 ml of the cell suspension was transferred to a fresh micro centrifuge tube and placed in liquid nitrogen until the cells were frozen followed by thawing at 37°C for a minute. The freeze/thaw cycle was repeated at least twice and 0.7 ml of Z buffer and β-mercaptoethanol (the mixture of Z buffer/β-mercaptoethanol was prepared by adding 0.27 ml of β-mercaptoethanol to 100 ml of Z buffer) was added to the reaction and blank tubes (blank tube was set up with just 100ml of Z buffer). 0.01M ONPG (Sigma, Oakville, ON) in Z buffer was added to the reaction and blank tubes and placed at 30°C. Once the yellow colour was developed, 0.4 ml of 1M Na_2CO_3 was added to the reaction and blank tubes and the elapsed time was recorded in minutes. The reaction tubes were centrifuged for 10 min at 13,400 g to pellet cell debris and the supernatants were transferred to clean cuvettes. The spectrophotometer was calibrated against the blank at A_{420} and the OD_{420} of the samples was measured relative to the blank and β-galactosidase units were calculated. 1 unit of β-galactosidase is defined as the amount, which hydrolyses 1 μmole of ONPG to O-nitrophenol and D-galactose per min per cell. β-galatosidase units = $1,000 \times OD_{420}/(t \times V \times OD_{600})$ where t = elapsed time (in min) of incubation, V= 0.1ml x concentration factor(5), $OD_{600} = A_{600}$ of 1ml of culture.

(viii) Plasmid isolation from yeast

In order to rescue the library plasmid DNA from yeast, each positive colony was grown in selection media (Leucine deficient media) overnight at 30°C. The culture was

placed in an eppendorf tube and spun at a high speed (13,400g) for a minute in a micro centrifuge at 4°C. The pellet was resuspended in 250 µl of resuspension buffer (Qiaprep kit, Qiagen, Missisauga, ON) which contained 50 mM Tris-HCl, pH8.0, 10 mM EDTA, pH 8.0 and 100 µg/ml RNase A). The yeast cells were disrupted by vortexing with acid-washed glass beads (Sigma,Oakville,ON) as the yeast cell wall is thick. To this, 250 µl of lysis buffer (Qiaprep kit, Qiagen, Missisauga, ON) containing 0.2 N NaOH and 1% SDS was added and the tube was gently inverted 4-6 times in order to mix and to this, 350 µl of N3 buffer (Qiaprep kit, Qiagen, ON) containing 3 M Guanidine-HCl, pH 4.8 was added and the tube was inverted immediately but gently 4-6 times and centrifuged at 13,400 g for 10 minutes at 4°C. The supernatant was applied to the column, and centrifuged for a minute at 13,400 g at 4°C. The flow through was discarded and the column was washed by adding 750 µl of PE buffer (10 mM Tris-HCl, pH 7.0 and 50% ethanol) (Qiagen, Missisauga, ON) and centrifuged for a minute at 13,400 g at 4°C. The flow through was discarded and the column was centrifuged for an additional minute to remove the residual wash buffer. The column was placed in a clean micro centrifuge tube and in order to elute the DNA, 25 µl of double distilled water was added to the column and centrifuged for a minute at 13,400g in a micro centrifuge at 4 °C. Once the plasmids were isolated from the yeast, they were transformed into *E.coli.*

(ix)Transforming E.coli with yeast plasmids:

1 µg of plasmid DNA isolated from the yeast was added to 100µl of chemically competent cells (Stratagene, La Jolla, CA) in a pre-chilled Falcon tube and mixed well by gently tapping. This transformation mix was then incubated on ice for 30 min. Cells were

then heat shocked at 42°C in a heat block (Brinkmann) for 30 sec and were then immediately transferred to ice for 2 minutes. 750µl of room temperature LB media was added and tubes were shaken at 250 rpm at 37°C for 1 hour (Eppendorf Thermomixer, Brinkmann). 100µl of the transformants was then spread onto pre-warmed LB agar plates with Ampicillin(100µg/ml) and amplified by a MidiPrep (Qiagen, Missisauga, ON). The clones from the library in pGADGH vector were verified by restriction enzyme analysis and sent for sequencing (CMRS, Ottawa). Nucleotide sequences were then compared against a sequence database (NCBI, BLAST) to identify the clones.

2.1(b) Affinity chromatography: Principle

Another approach of finding the interacting proteins of Mfn2 was to perform an affinity column using Mfn2 (710-757) as bait. The principle is shown in Figure 8. The bait protein, Mfn2 (710-757) fused to GST (GST: Mfn2 (710-757)), was expressed recombinantly, bound to sepharose beads and washed by PBS extensively. The lysates from both cytosol and solubilised mitochondria from human placenta were used as the source. The lysates were prepared and then incubated with empty glutathione sepharose beads to remove any non-specific proteins binding to the sepharose beads. Then the lysate was incubated with the (GST:Mfn2 (710-757)) beads and the columns were washed extensively, and the bound products are selectively eluted by cleaving Mfn2(710-757) from GST on the column with thrombin. Fractions are collected and analysed by SDS-PAGE.

Figure 8: Principle of Affinity Column:

The bait protein, $Mfn2_{(710\text{-}757)}$ is purified from bacterial lysates by affinity chromatography using glutathione sepharose beads and incubated with the lysate of choice and eluted by cleavage with thrombin. Non-specific proteins (D) remain bound to the beads and proteins interacting with the bait are eluted.

1. Purification of GST fusion bait protein Mfn2 (710-757)

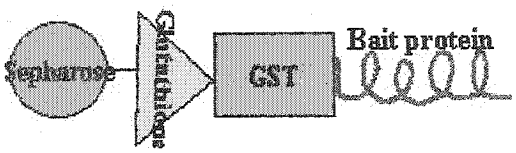

2. Incubation of purified protein with lysate

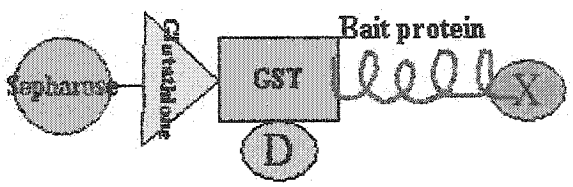

3. Elution by cleavage with thrombin

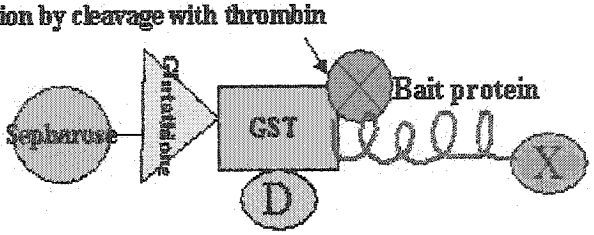

4. Non specific proteins remain bound to the sepharose beads and proteins interacting with the bait are eluted

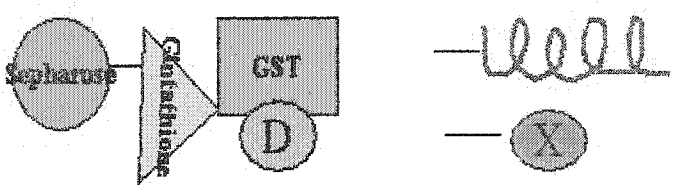

(i) Preparation of the construct

Full-length human Mfn2 (1-757) pcDNA3.1+ was digested with Sma/Xho1. The resulting nucleotide fragment (141 bp) was excised for ligation into pGEX-4T3 vector (Clontech, Palo Alto, CA) cut with Sma1/Xho1 for protein expression and thrombin cleavage in order to obtain Mfn2 (710-757), which is a short-coiled coil domain. This was purified using a GST fusion system.

(ii) Expression and purification of GST: Mfn2 (710-757) and GST

BL21 cells (Stratagene, LaJolla, CA) were transformed with Mfn2 (710-757)-pGEX4T3 and pGEX4T3 alone was used as a control. The transformed bacteria were grown in LB-ampicillin medium at 37° to a cell density of OD600 = 0.7 in a volume of 9 litres. The culture was induced with 0.3 mM IPTG (isopropylthiogalactoside) for 2 hrs. The cells were harvested in 750 ml buckets at 4000 g for 15 min at 4°C (using SORVALL LEGEND RT centrifuge with a fixed angle rotor) and the cell pellet was resuspended in 100 ml of 1X phosphate buffered saline (1X contained 40 g Nacl, 1 g Kcl, 7.2 g Na_2HPO_4 and 1.2 g KH_2PO_4 (pH7.4) and frozen at -20°C. The bacteria were thawed and 5 mM β-mercaptoethanol (OmniPur, Darmstatd) and 1X protease inhibitors (60μg/ml chymostatin, 1.1×10^{-6} M leupeptin, 2μg/ml aprotinin, 25μg/ml antipain, and 1×10^{-3} M pepstatinA) were added and lysed using a French Press at 1500-2000psi. The lysate was cleared at 90,000 g for 25 min at 4°C in a Beckmann ultracentrifuge using Ti70 rotor. The supernatant was incubated with glutathione sepharose beads (Amersham Pharmacia, Piscataway, NJ) pre-equilibrated with PBS (phosphate buffered saline) and incubated at

4°C for 2 hrs rotating. The unbound proteins were washed with PBS buffer containing 2 mM βME, 10 mM $MgSO_4$ and 2 mM ATP. The protein concentration was determined (Bio-Rad protein assay, Bio-Rad, Hercules, CA) by taking 10 µl of beads eluted in elution buffer containing 50 mM Tris pH 8.0; 150 mM NaCl and 15 mM reduced Glutathione (Sigma, St.Loius, MO).

(iii) Preparation of placental mitochondrial extracts

Human placenta was obtained from the Heidelberg Women's Hospital (Heidelberg,Germany), within two hours after birth and placed immediately on ice for transport to Ottawa. All manipulations were subsequently carried out at 4 °C. Umbilical cords were removed along with excess sac material and the placenta was minced with scissors. The minced material was washed with PBS to remove blood and the final two washes were done in 250 mM sucrose, 3 mM imidazole, and 1mM MgCl2 pH 7.4. The final volume of buffer:placenta was 1:1 and protease inhibitors (as mentioned above) with 1 mM DTT (Dithiothreitol)(Sigma, Oakville, ON) were added. The material was placed in a Waring blender on high speed until smooth (15 min). The broken cells were then centrifuged in a GS3 rotor at 8000 rpm (~10,000 x g) for 30 minutes to remove unbroken cells, connective tissue and nuclei. The supernatant of this spin was then placed in a GSA rotor and centrifuged at 10,000 g for 20 minutes at 4°C. The pellet was kept as the mitochondrial fraction and resuspended in 10 mL of 250 mM sucrose, 3 mM imidazole, 1 mM $MgCl_2$, pH 7.4, aliquoted into 2 mL tubes, snap frozen in liquid nitrogen and stored at –80°C. For use in the affinity column, mitochondria (120mg mitochondrial protein) were thawed and adjusted to 1% Triton X-100, incubated by

rotation at 4°C for 2 hours to solubilize the membranes. Then the solubilized material was centrifuged in the TLA100.4 rotor in a Beckmann centrifuge at 267,000 g for 30 minutes to remove the insoluble material. The supernatant was taken as the soluble mitochondrial fraction and calculated to contain ~10 mg/ml protein. Prior to use in the affinity column, the mitochondrial lysate was preincubated with equilibrated glutathione sepharose beads to reduce the non-specific background proteins from binding to the column. For this, ~600 µl packed beads were incubated with 6 mL lysate for 1 hour at 4°C under rotation. Following this, the lysate was centrifuged in a low speed centrifuge for 10 minutes at 3000g. The supernatant was kept as pre-cleared lysate for use in the column and the beads were discarded.

(iv)Preparation of cytosol

Spinner culture adapted sHeLa cells were seeded in a spinner flask containing a litre of s-MEM (Gibco, Tulsa, OK) at a density of 10^4cells/ml and grown in suspension for 4 days. Then 5 x 10^8 cells/L from spinner culture were centrifuged at 150 g. The cell pellet was washed once with PBS, then resuspended in 5 ml KEHM buffer (50 mM KCl, 50 mM Hepes, pH 7.4, 10 mM EGTA, 2 mM $MgCl_2$) containing the protease inhibitors as mentioned above. The cells were then broken in an 8.020 mm cell-cracking chamber with a ball bearing sized 8.004 mm. The cell lysate was centrifuged at 750 g (SORVALL LEGEND RT centrifuge with fixed angle rotor) for 5 min at 4°C to remove nuclei. The supernatant was recovered and centrifuged again at 100,000g (in a tabletop ultracentrifuge using a TLA100.4 rotor) for 30 min at 4°C to obtain the cytosolic fraction. The supernatant was recovered and aliquoted and frozen in liquid nitrogen for storage at –80 °C.

(v)Affinity column for identifying the interacting proteins

Once the protein concentration for both the constructs (Mfn2 (710-757) and GST) was found (which was approximately 5 mg), each column was incubated with solubilised mitochondrial lysate (30 mg of protein) or cytosolic lysate (30 mg of protein) for 2 hrs with rotation at 4°C. These columns were washed extensively with 10 column volumes of wash buffer which contained 20 mM Hepes pH 7.4, 250 mM NaCl, 2 mM $MgCl_2$, 2 mM β-mercaptoethanol and the bound proteins were selectively eluted by cleaving the Mfn2 (710-757) coil (which was 5Kda) from the GST on the column with 0.2 NIH units of thrombin/μg for 1 hour at room temperature (One cleavage unit digests ≥ 90% of 100μg of a test protein in 16 hours at 22°C in elution buffer, a cleavage unit is approximately equal to 0.2 NIH units). The fractions were collected and the beads were washed twice with wash buffer as mentioned above and finally the remaining GST was eluted with 3 column volumes using 50 mM Tris pH8.0, 15 mM reduced Glutathione and 150 mM NaCl. The protein concentration was checked in all fractions using Bio-Rad protein assay and analysed by SDS-PAGE stained with Coomassie blue.

2.2 Dissection of role of Mfn2:

This study hopes to understand the mechanism of mitochondrial fusion by dissecting the role of Mfn2 in this process.

2.2 (a) Preparation of constructs:

Mitofusin2 cDNA was first excised with Afl11 and Apa1 and inserted into mammalian expression vector pcDNA3.1+. The amino terminal end of Mfn2 was PCR amplified (Cloned Pfu Polymerase, Stratagene, LaJolla, CA) using a sense primer containing a 5'

BamH1 restriction site and an antisense primer for amplification through the NheI site for digestion and insertion into the pcDNA3.1:$Mfn2_{(30-560)}$ plasmid. The carboxy terminal end of Mfn2 was PCR amplified with a sense primer to amplify the AflII site, and antisense primer containing a 3' HindIII site for insertion into digested pcDNA3.1:$Mfn2_{(1-560)}$ to obtain the full length pcDNA3.1:Mfn2. The full length Mfn2 cDNA was then subcloned into pECFP-C1 (Clontech,Palo Alto,CA) using BamH1 and HindIII restriction sites. $Mfn2_{(430-757)}$CFP was created by digesting Mfn2pcDNA3.1+ with Sal1 and HindIII and inserted into pECFP-C1 cut with Xho1 and HindIII. Mfn2RasG12VCFP was prepared using Quick-Change mutagenesis (Stratagene,LaJolla, CA) using pECFP-C1:Mfn2 as the template and a set of oligonucleotides designed to replace amino acids GRTSNGKS with GAVGVGKS. The restriction site Nar1 was introduced into the primers for screening purposes. pcDNA3: pOCT-YFP, pcDNA3:pOCT-GFP contain the cleavable 32 amino acid mitochondrial matrix targeting signal of ornithine carbamyl transferase (Nguyen et al., 1986) fused in frame to YFP and GFP respectively and was gratefully obtained from John Silvius at McGill University, Montreal, Quebec. The cDNA encoding DsRed2 was amplified from the Clontech (Palo Alto, CA) vector pDsRed2-C1 using primers 5'-cg gga tcc atg gcc tcc tcc gag aac gt-3' and 5'-gc tctaga gcggccgc tta cag gaa cag gtg gtg gcg gc-3' for digestion with BamH1 and Xba1. The cleaved DsRed2 cDNA was ligated into the pcDNA3: pOCT-GFP vector digested with BamH1 and Xba1 following removal of the GFP cDNA by agarose gel purification. All sequences were confirmed by sequencing and no other mutations were introduced in the PCR mutagenesis.

2.2 (b)Transfection and imaging of Cos7 cells

Cos7 cells were grown on glass coverslips in 24 well plates to ~70% confluence in Dubecco's Modified Eagles Medium (DMEM) supplemented with 10% fetal calf serum, 100 μg/ml penicillin and 100 μg/ml streptomycin sulfate (Gibco,Tulsa ,OK) before transfection with Lipofectamine 2000 (GIBCO,Tulsa,OK). For imaging, coverslips were removed and placed in an aluminium slide chamber (EMBL, Heidelberg) with Hepes buffered complete DMEM, pH 7.4, maintained at 37 °C. Images were taken with an Olympus 100X U Plan Apochromat, NA 1.35 – 0.50 objective on an Olympus IX70 inverted microscope equipped with a 12 bit IMAGO SVGA CCD camera and the Till Polychrome IV monochrometer (T.I.L.L. Photonics GmbH) controlled by TillVisION v. 4.0 software. CFP tagged proteins were excited at 434 nm and YFP at 514 nm using the CFP/YFP Dual set (T.I.L.L. Photonics, GmbH) and Mitofluor Red 589 dye was excited at 589nm using CFP/YFP/DsRed triple pass filter. Switching between wavelengths took 3 msec, and exposure times were typically between 100-500 msec. For co-transfection experiments, images were merged as RGB and converted to 8 bit in the TillVisION software and exported as .tiff files for further processing with Adobe Photoshop. For PEG Fusion assay, live cells were imaged on the Olympus IX70 microscope with a 100X objective, exited at 488 nm (GFP) and 560 nm (DsRed2) with the Polychrome IV monochrometer (TillPhotonics, Gräfelfing, Germany) through a FITC/Cy3/Cy5 triple pass filter (Chroma, Battelboro, VT). The emitted light was filtered through an additional Dual-View beam splitter (Optical Insights, Santa Fe, NM) equipped with two filters of HQ520-20 and D600/40 to separate the GFP and DsRed2 emission signals, and images were captured using an sVGA IMAGO CCD camera integrated with the TillVisIon

software. The transfected CFP tagged protein was imaged using the CFP/YFP dual pass filter (TillPhotonics) along with the beam splitter equipped with D465/30 and HQ535/30 filters. The acquired images were saved as .tiff images and overlayed in Adobe Photoshop for image assembly. For TMRE flickering experiments, 50 nM TMRE (Sigma, Oakville, ON) was added to the chamber medium and incubated with the cells at 37 degrees for 20 minutes. Following equilibration of the dye, 100 images were collected by exciting at 549 nm with the FITC/Cy3/Cy5 triple pass filter (Chroma, Vermont) for 500 msec followed by a 1000 msec delay. Time series were cropped if necessary, converted to 8 bits using TillVision software and exported as .avi files.

2.2 (c) Mant GMP-PNP binding assay:

COS-7 cells (grown in 10cm dishes) were transfected with pOCT-CFP, Mfn2CFP, $Mfn2_{RasG12V}$CFP, and Rab5CFP fusion constructs. The day after transfection, the cells were harvested by trypsinization, washed with PBS, and with nucleotide binding buffer (220 mM mannitol , 68 mM sucrose, 2 mM NaCl, 2 mM $MgCl_2$, 0.5 mM EGTA, 2.5 mM KH_2PO_4, 10 mM Hepes, pH 7.4, 1mg/ml BSA) containing protease inhibitors. Cells were then broken in a cell cracker, and the whole lysate centrifuged at 9,300 g, to concentrate heavy membrane fractions. Pellets were resuspended in binding buffer and 50 µl aliquots were mixed with Mant-GMP-PNP (1 µM final conc., Molecular Probes, Oregon) and incubated at 37 °C for different times. After incubation the aliquots were scanned for emission fluorescence of Mant-nucleotides in a QuantaMaster 6000SE spectrofluorometer from Photon Technology International (excitation at 360 nm). The peak emission at 448 nm was recorded and the background fluorescence of the nucleotide alone was subtracted. Each value was also normalized for total protein concentration in

the sample (determined using the Bio-Rad protein assay (Biorad)), and for the level of recombinant protein expression by measuring the CFP signal obtained in the fluorimeter upon excitation at 434 nm, emission at 477 nm.

2.2 (d) Effect of nocodazole on the clustered mitochondria

Cos7 cells (as described in sub section 2.2(b)) were co-transfected with galatosyltransferase:YFP (obtained from Dr.Zemin Yao, University of Ottawa Heart Institute) in order to label the Golgi and CFP-Mitofusin2 (or CFP-Mitofusin2 Pact or Mfn2(430-757) using Lipofectamine 2000 (mentioned in the subsection 2.2(b) and after 16 hours following transfection, 20μM nocodazole (Sigma,Oakville,ON) in DMSO was added for 6 hours and the cells were imaged. Mitochondria were labelled with 100nm concentration of Mitofluor Red (Molecular Probes, Eugene, OR).

2.2 (e) PEG Fusion Assay

The whole cell fusion assay was performed essentially as described recently (Legros, 2002). Briefly, 10 cm dishes of COS7 cells were transfected with 1-3 μg of Mfn2CFP: pOCT-DsRed and Mfn2RasG12V-CFP: pOCt-DsRed for 8-10 hours using the Lipofectamine 2000 reagent (Invitrogen), followed by trypsinization, and mixing of equal cell numbers of pOCT-GFP transfected cells with each pOCT-DsRed co-transfections. Each mixture of pooled cells were plated into a 1 cm well containing a glass coverslip, and seeded overnight. After 12 hours, 30ug/ml cycloheximide was added to the medium in order to chase the recently synthesized marker proteins into the mitochondria and to arrest any further translation. Following the incubation in cyclohexamide containing media, cells were washed 2 times with PBS and 200 μL of 50% PEG 5000 (Sigma,

Oakville) was added for 60 seconds. Cells were immediately washed three times with PBS and then incubated with fresh media containing 30 μg/ml cycloheximide, and mounted in aluminum slide chambers (EMBL-Heidelberg) for imaging. The schematic representation of this method is shown in Figure 9.

2.2 (f) Electron Microscopy of the fused and clustered mitochondria

Cos7 cells were transfected with Mfn2: CFP, Mfn2RasG12V and Mfn2(430-757) in separate 10 cm dishes with Lipofectamine 2000 for 16 hours. Following this, fluorescence was first examined using the light microscope to ensure transfection was at least 70% prior to trypsinization and washing of the cells in PBS. The washed cells were then pelleted and fixed in 1.6% glutaraldehyde (Marivac, Montreal) in 0.1M Na Cacodylate buffer (Marivac, Montreal) prior to osmium tetroxide and uranyl acetate staining, spurr resin embedding and final thin sectioning of the blocks. Grids were stained with lead citrate (Marivac, Montreal) and images were subsequently taken in a Hitachi 7100 at 20 - 50,000X magnification. Negatives were developed, scanned using an AGFA Arcus 1200 at 600 dpi and imported into Adobe Photoshop for assembly into figures.

Figure 9: Schematic representation of PEG fusion assay:
Polyethylene glycol (PEG) fusion assay was used to test for fusion in various Mfn2 constructs. Shown in blue are the cells transfected with Mfn2CFP, Shown in red are the cells transfected with pOCT-DsRed to label the mitochondria and shown in green are the cells transfected with pOCT-GFP to label the mitochondria. Yellow indicates that there is mixing between green and red indicating fusion.

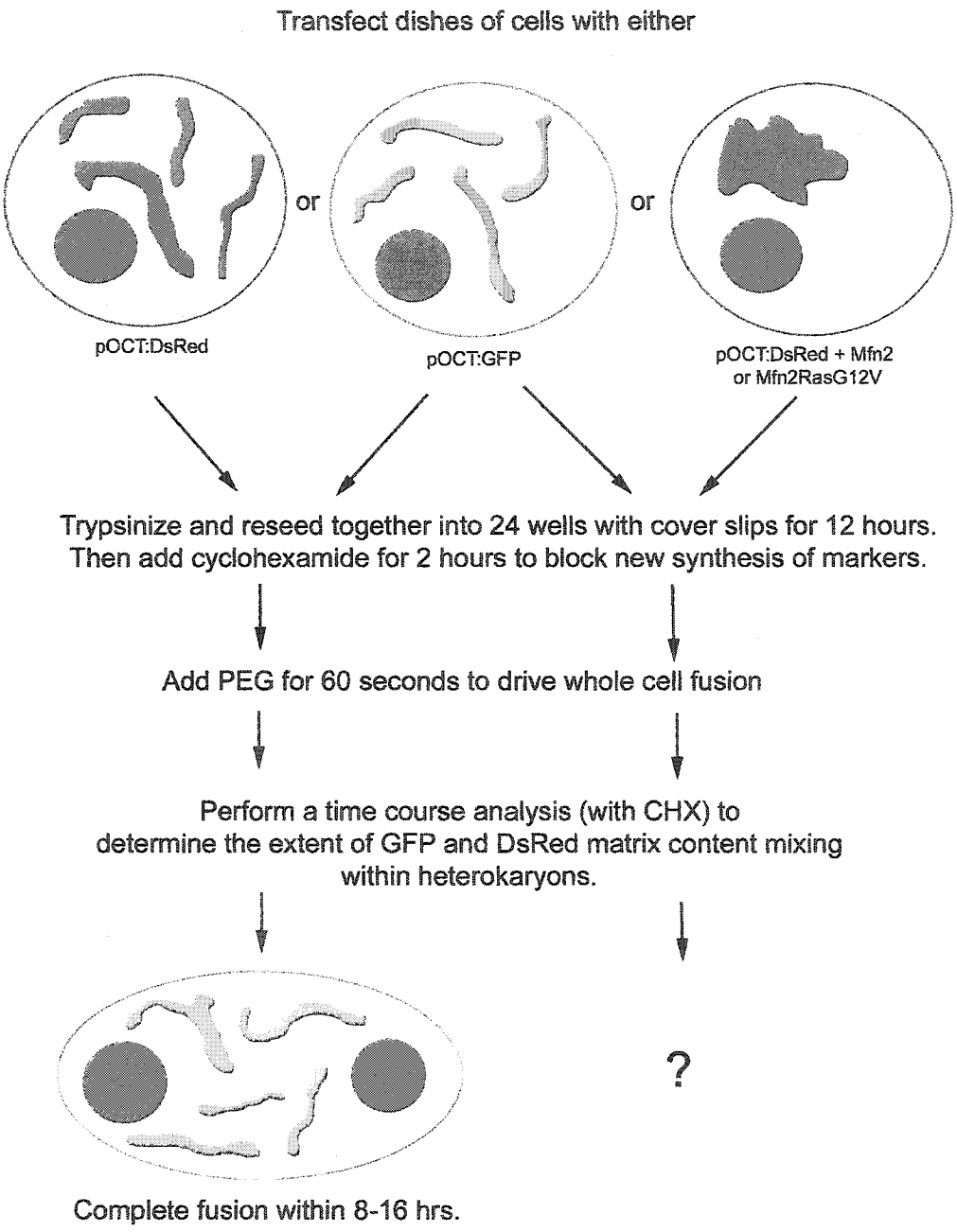
Transfect dishes of cells with either
or
or
pOCT:DsRed
pOCT:GFP
pOCT:DsRed + Mfn2
or Mfn2RasG12V
Trypsinize and reseed together into 24 wells with cover slips for 12 hours.
Then add cyclohexamide for 2 hours to block new synthesis of markers.
Add PEG for 60 seconds to drive whole cell fusion
Perform a time course analysis (with CHX) to
determine the extent of GFP and DsRed matrix content mixing
within heterokaryons.
?
Complete fusion within 8-16 hrs.

3. Results

3.1 Identifying interacting proteins:

One of the objectives of this study was to identify the interacting proteins of Mfn2 to understand the mechanism of mitochondrial fusion.

3.1 (a) Yeast two-hybrid screen:

One of the methods employed to identify the interacting proteins was yeast two-hybrid screen. The predicted soluble GTPase domain of Mitofusin 2 (Mfn2 (1-560)) ligated into the pLexA vector in-frame with pLexA DNA binding domain was used as a bait to search for proteins expressed by a HeLa cDNA library encoding the activation domain of pGAD vector. HeLa library in pGADGH vector was obtained gratefully from Dr.Marino Zerial and was chosen because wide range of proteins might be tested which are specific for mammals.

(i) pLexA-Mfn2(1-560) is expressed at low levels in yeast.

pLexA-Mfn2(1-560) transformed yeast grew only on tryptophan deficient plates (tryptophan is expressed from pLexA plasmid) and not on tryptophan, leucine and histidine deficient plates which confirmed that there is no auto-activation of the reporter genes. Before proceeding to the actual screen, the actual expression of the pLexA-Mfn2 (1-560) inside yeast was verified by a Western blot (see Figure 10). The controls used were pLexA alone and Rab5Q79L. The OD600 recorded for 1ml of yeast cultures of pLexA-Mfn2(1-560), pLexA and Rab5Q79L were 1.6200, 1.3800 and 1.6140 respectively. In order to obtain approximately the same amount of cells, 6ml

Figure 10: Western blot verifying the expression of pLexA-Mfn2 in yeast. Approximately the same amount of cells of pLexA-Mfn2(1-560), Rab5Q79L and pLexA were used for protein extraction. The samples were boiled for 5 minutes and loaded on a gel. As shown in the figure, the expected size of pLexA-Mfn2 is ~ 90Kda. Also shown are expressions of Rab5Q79L used as a positive control and pLexA alone.

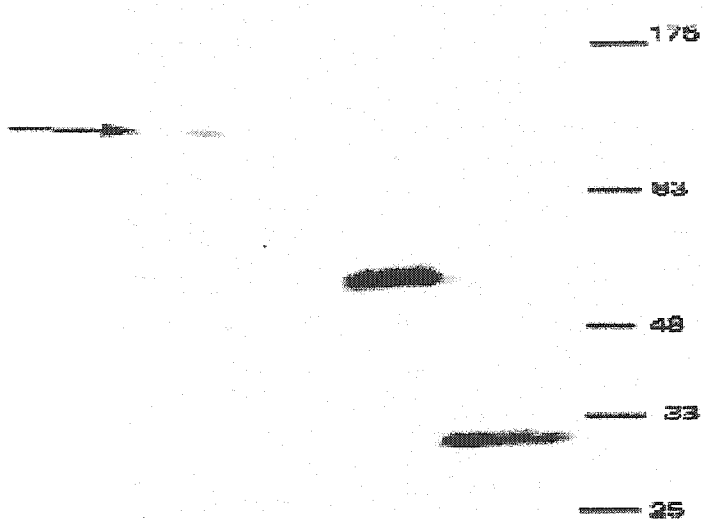

Mfn2 Rab5Q79L pLexA

(OD600=9.72), 7ml(OD600=9.66)and 6 ml(OD600=9.68) cultures of pLexA-Mfn2(1-560), pLexA and Rab5Q79L were used and the protein extracts were prepared by Urea/SDS method as discussed in the section 2.1(iv). The protein samples were boiled for 2 minutes at 80°C in a multi-block heater and loaded on the gel. The expected sizes of pLexA-Mfn2(1-560), pLexA alone and Rab5 were ~90 Kda, ~30 Kda and ~60 Kda respectively. The expression level of pLexA-Mfn2(1-560) was at least 50 times less than that of the controls.

(ii) Transformation efficiency was found to be 1×10^4colonies/μg of library DNA.

Once it was known that the pLexA-Mfn2(1-560) fusion construct was expressed in the yeast, the transformation efficiency of the library plasmids was calculated by transforming yeast already containing the LexA: Mfn2 (1-560) plasmid and examining the number of colonies growing per μg library DNA transformed. By plating the transformed yeast cells in dilutions of 1:100000, 1:10000 and 1:1000 on -Trp,-Leu plates, the efficiency was found to be ~$1x10^4$ transformants/μg of library DNA. Therefore a 60X reaction was performed in order to screen the whole library (6 x 10^6 colonies). The efficiency was not as high as expected during the scale up because only $1x10^6$ clones for 60μg of library DNA were screened as opposed to 6.6 x 10^6 clones in the library.

(iii) Three clones from the HeLa library were identified to be interacting with pLexA-Mfn2 (1-560).

Among $1x10^6$ clones, 300 colonies grew on –Trp,-Leu,-His plates and among them only 7 turned blue on a colony lift filter assay (see Table 1). A quantitative β-Gal liquid assay was performed on the positive clones where only 3 clones had no problem in growth in the liquid media but the rest did not grow. The ODs recorded at OD600 for clones numbered 1 to 7 were 0.4553, 0.023, 0.032, 0.0042, 0.011, 0.4961, 0.1550 respectively. Only clones numbered 1, 6 and 7 were considered. The β-Galactosidase units were calculated by the formula mentioned in the methods for quantitative β-Galactosidase assay and the units for the positive clones were found to be nearly 200 times less than the positive control, which was the interaction between, activated Rab5Q79L and Rabaptin5 (see Table 2). The relative β-galactosidase units of the positive clones were plotted and the units were found to be almost negligible when compared to the positive control (see figure 11). The 3 positive clones were sequenced which were Homeobox C10 (obtained twice in the screen) that is a developmentally regulated protein (Gardiner DM, 2001) and a Heterogenous nuclear ribonucleoprotein which is a previously reported false positive (Serebriiskii, 2000)

Table 1: Summary of the results of yeast two-hybrid screen

Full Library	6.6×10^6
Clones screened	1.5×10^6
Isolates	300
Positive clones	3
Sequenced	3
Clones	Homeobox C10 (2)
	Heterogeneous ribonucleoprotein

Table 1: Summary of the results of two hybrid screen: The number of clones screened were 1.5×10^6 clones as opposed to 6.6×10^6 clones in the library and isolated 300 clones which grew on –Trp,-Leu,-His plates and among them 7 turned blue on a colony lift filter assay. A quantitative β-Gal liquid assay was performed on the positive clones where only 3 clones had no problem in growth in the liquid media but the rest didn't grow. 3 positive clones were sequenced (Canadian Molecular Research Services, Ottawa) which were Homeobox C10 (obtained twice in the screen), a developmentally regulated protein (Gardiner DM, 2001) and a Heterogenous nuclear ribonucleoprotein, which is a previously reported false positive.

Table 2: Quantification of β-galactosidase activity

Clones	O.D	Cells/ml	Absorbance at420nm	β-Galactosidase units
1	0.4553	0.94×10^{7}	0.1346	1.363×10^{-7}
6	0.4961	0.99×10^{7}	0.1295	1.3×10^{-7}
7	0.1550	0.28×10^{7}	0.0708	0.2107×10^{-7}
Rab5 (Q79L) and Rabaptin	0.8	1.7×10^{8}	0.5473	32.19×10^{-8}

Table 2: Quantification of β-galactosidase activity: The interactions between Mfn2 and the clones which turned blue in colony lift filter assay were confirmed by a quantitative liquid β-galactosidase assay. For this, the yeast with the respective clones were grown in synthetic media lacking tryptophan,leucine and histidine and then incubated at 30°C for 3-5 hrs until the cells were in mid-log phase and the O.D at 600nm was recorded when the cells were harvested. The β-galactosidase activity was determined as described in the materials and methods. As a positive control, the interaction between Rab5 and Rabaptin was used. β-Galactosidase units for clones 1,6 and 7 were very low when compared to the interaction between Rab5 and Rabaptin

Figure 11: Relative β-Gal Assay of yeast two hybrid positive clones:
The relative β-galactosidase units of the positive clones obtained in the liquid β-galactosidase assay (numbered 1, 6 and 7)were plotted and the units were found to be almost negligible when compared to the interaction between Rab5 and Rabaptin (the relative β-galactosidase units were 300).

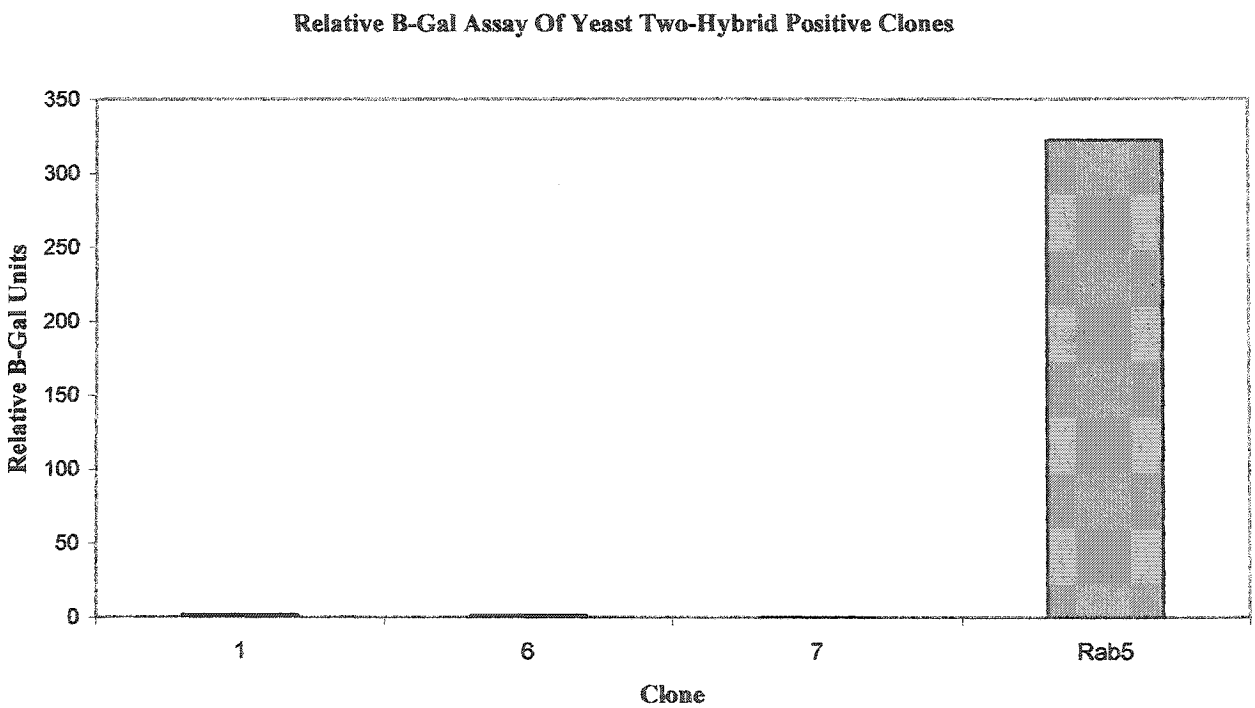
Relative B-Gal Assay Of Yeast Two-Hybrid Positive Clones
Relative B-Gal Units
350
300
250
200
150
100
50
0
1
6
7
Rab5
Clone

3.1 (b) Affinity column

Morphological studies revealed that the carboxy terminal coiled region dominantly interferes with the endogenous function of the protein (see results of dissection of role of Mfn2). This dominant interfering phenotype led us to hypothesise that the carboxy terminal coiled domain may be interacting directly with other proteins responsible for mitochondrial fusion. In order to test this directly, we designed an affinity chromatography using recombinant Mitofusin2 (710-757) that was purified using GST fusion system.

(i) Purification of Mfn2(710-757)

The GST fusion construct with Mfn2(710-757) was first expressed recombinantly and the bacteria were pelleted and resuspended in PBS and two microlitres were run on the gel (Figure 12, lane 1). A French cell Press was used to break open the bacteria and the lysate was cleared (Figure 12,lane 2) and 2 microlitres of the pellet were saved for the gel (Figure 12, lane 3). The GST:Mfn2(710-757) was then bound to glutathione sepharose beads and the supernatant was carefully poured off (flow through),(Figure 12, lane 4) an the beads were washed extensively (Figure 12, lanes 5,6 and 7). This was followed by 3 elutions (figure12, lanes 8,9 and 10) and also 10 microlitres of beads were run on the gel to know how much of GST:Mfn2(710-757) was remaining after elution (Figure 12, lane 11). The protein concentration was determined using Bio-Rad protein assay. As expected the size of GST:Mfn2 (710-757) was ~30Kda. Finally the 5Kda Mfn2 (710-757) was cleaved using thrombin (figure 12, lane 12) and the yield was 5 mg.

Figure 12: Purification of Mfn2(710-757) by GST fusion system.
The GST fusion construct with Mfn2(710-757) was expressed recombinantly and the bacteria were pelleted and resuspended in PBS and two microlitres were run on the gel (total). A French cell Press was used to break open the bacteria and the lysate was cleared (supernatant) and two microlitres of the pellet were saved for the gel (pellet). The GST:Mfn2(710-757) was then bound to glutathione sepharose beads and the supernatant was carefully poured off(flow through) and the beads were washed extensively (Wash 1,2 and 3). This was followed by 3 elutions and also ten microlitres of beads were run on the gel to know how much of GST:Mfn2(710-757) was remaining after elution. The protein concentration was found be 10mg. As expected the size of GST:Mfn2(710-757) was 30Kda. Finally the 5Kda, Mfn2(710-757) was cleaved using thrombin.

Total
Supernatant
Pellet
Flowthrough
Wash 1
Wash 2
Wash 3
Elution 1
Elution 2
Elution 3
Mfn2 (710-757)-GST
Mfn2 (710-757)
148
98
64
50
36
22
16
6
5 Kda, Mfn2 (710-757)

(ii) Affinity column with GST:Mfn2(710-757)

The affinity chromatography was performed using recombinant GST: Mitofusin2 (710-757) as bait. The experiment was dome twice and the difference was that 1mg of the recombinant protein was used instead of 5 mg as used previously, the amount of the protein in mitochondrial lysate was 10 mg as opposed to 30 mg used in the first experiment, and the cytoslic source for proteins was not used in the second experiment. One more important difference was that in the second experiment, the mitochondrial lysate was precleared by incubating with empty glutathione sepharose beads in order to remove non-specific binding to the beads. In order to determine how much of the bait and how much of lysate has to be used, a number of starting assumptions were made. First, it is likely that much of the recombinantly expressed protein is not fully capable of engaging in protein interactions, so it was assumed that about 1 in 1000 of the bait molecules would bind competently for various reasons. The objective of the experiment was to obtain enough of the interacting partner to be able to send it for MS/MS sequencing, which would be between 1-5 μg protein. If we assume that most proteins represent only 0.01% of total lysate proteins, then to get 1-5 μg of protein, at least 10-50 mg lysate would be needed. So we used at least 5 mg of the bait and 30 mg of lysate. At least 7 specific proteins were retrieved from mitochondrial lysates and interstingly there were no cytosolic proteins found on the column incubated with cytosol (Figure 13) and the identification of bands is shown in Table 3.

Figure 13: Affinity column with GST:Mfn2(710-757).
GST:Mitofusin2$_{710\text{-}757}$ containing only the carboxy-terminal coiled coil region was expressed in bacteria and used as bait to identify interacting proteins. Each column contained 5 mg of recombinant protein and was incubated with ~30 mg of either cytosol prepared from HeLa cell lysates, or 30 mg of mitochondrial lysate purified from human placenta. GST alone was used as a negative control. The recombinant GST fusion proteins were bound to Glutathione-Sepharose beads, then incubated with the lysates (as indicated). Following washes, bound proteins were eluted by cleaving the 5 kDa mitofusin2$_{(710\text{-}757)}$ and leaving the GST protein on the Glutathione Sepharose beads. The full commassie blue stained gel is shown along with a magnified section containing a number of bands specific to the mitochondrial lysate. In the first experiment, 4-20% gel had 4 strong background bands, but specific bands were visible. Bands were not found using cytosol as source and were only mitochondria specific. The second experiment was much cleaner as most of the background was removed. The staining was low but the bands were still visible.

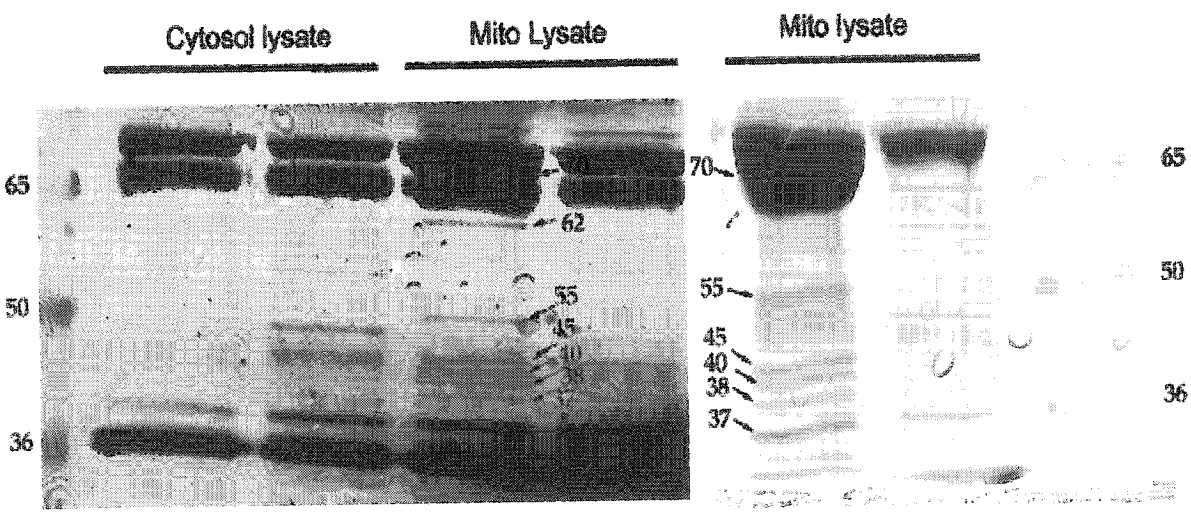
Cytosol lysate
Mito Lysate
Mito lysate
65
50
36
70
62
55
45
40
38
37
Mfn2(710-757)
GST
Mfn2(710-757)
GST
Mfn2(710-757)
GST
First Experiment
Second Experiment

Table 3. Identification of bands of the affinity column

MW*.	Species Id.	Mass Spec Peptides	Identity	Comments
p70	1	Not specified by SLI	HSP70	
p62	1	4 peptides (not specified by SLI)	Catalase	Peroxisomal
p55	1	LAFPFGIPNDPMLWSEGQSHLCWR	No redundant gi number.	homology to Rab27 effector myosin linker.
	2	TGLQAGLTIDEFAPR	methylmalonyl coA mutase	mitochondrial matrix enzyme
		GDVGmAGVAIDTVEDTKILFDGIPLEK	methylmalonyl coA mutase	
		DTMDLPEELPGVKPFTR	methylmalonyl coA mutase	
p45	1	not specified by SLI	GST	probably leakage from the column
	2	YGTLFTMDRVLTPPMGTVMDVLD	gi:299636 and gi:4507467	TGF beta induced message identified in array screen.
		VLTPPmGTVmDVLK	gi:299636 and gi:4507467	TGF beta induced message identified in array screen.
	3	RPVDSSPASEQRLPVLLWGLVEGLR	No redundant gi number.	completely unknown
		ASSFAmEPVLLSAEEAVQK	No redundant gi number.	
	4	AAQHAAAR	No redundant gi number.	completely unknown
		MAPGCEHEK	No redundant gi number.	
p40	ND			
p38	ND			
p37	ND			

Table 3: Identification of bands: The bands obtained from the column were cut and sent for M/S analysis to Samuel Lunenfield Research Institute (SLRI). The bands identified so far are shown in the table and the lab will investigate the characterization of the bands.

* Approximate Molecular Weight

** Species Identification

3.2 Dissecting the role of Mfn2 in mitochondrial fusion:

The second approach employed in order to understand the mechanism of mitochondrial fusion was to dissect the role of Mfn2 in this process by morphological and biochemical studies.

3.2 (a) Mitochondrial fusion is completed within 3-4 minutes.

In order to understand the events required to fuse two mitochondria, the details of single mitochondrial fusion events were examined under steady state conditions. To do this, the mitochondria were labelled by transfecting Cos7 cells with a mitochondrial marker YFP protein, pOCT-YFP. Following 16 hours of transfection, the glass cover slips were transferred to the video chamber and images were taken every 2 seconds for 400 frames. Within this short time span, we could easily observe extensive fusion and fission events throughout the cell. After imaging over 30 cells, at least 2-5 fusion events were observed per cell over a 3-4 minute time period, demonstrating the extremely dynamic activity of the mitochondria. The details of one of these fusion events are shown in Figure 14 and supplemental movie 1 on CD).

3.2 (b) Mfn2 is localized to specific subdomains along mitochondrial tubules when nucleotide exchange activity is low.

The nucleotide exchange properties of the P-loop mutation ($Mfn2_{RasG12V}$) were tested using crude extracts from cells transfected with CFP fusion proteins. Cos7 cells were transfected with either matrix targeted CFP (negative control), wild type Mfn2CFP,

Figure 14: Capturing mitochondrial fusion events:
COS7 cells transfected with pOCT-YFP were imaged with an Olympus IX70 microscope outfitted with a 100X objective every 2 seconds for 400 frames. YFP was excited at 500 nm using the Polychrome monochromator from TillPhotonics with the YFP filter set (Chroma) and the IMAGO CCD camera (Till). Cropped images of a single fusion event are shown taken at the time points indicated. Arrowheads point to the mitochondrial fusion events. Scale bar represents 1 μm. Video1 in the supplementary online materials shows all the frames taken in this time sequence.

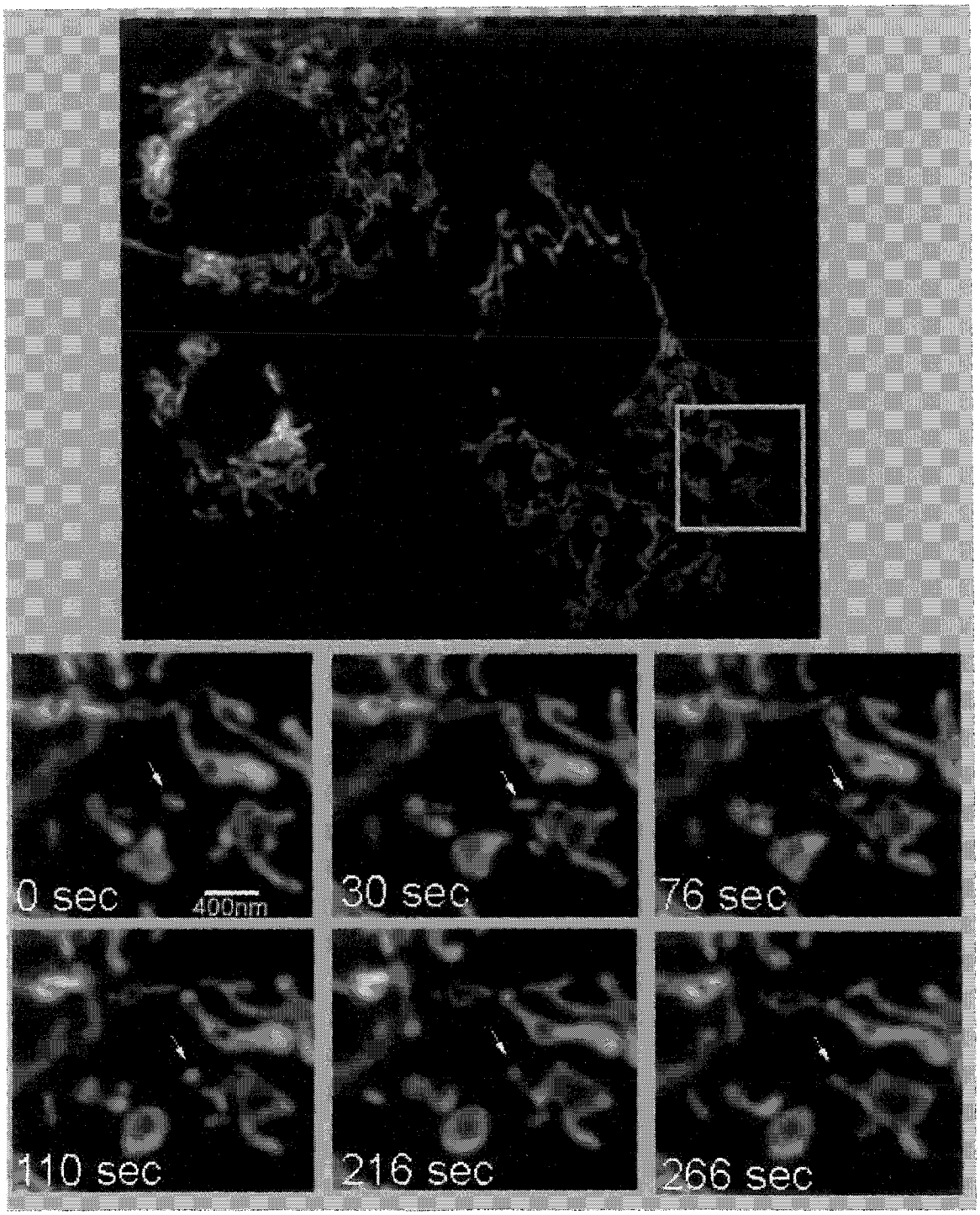
0 sec
400nm
30 sec
76 sec
110 sec
216 sec
266 sec

$Mfn2_{RasG12V}$CFP or Rab5CFP as a positive control. Following 16 hours of expression, the cells were harvested, broken, and incubated with the environment-sensitive non-hydrolysable GTP analogue, N-methylanthraniloyl-5'-guanylyl-beta,gamma-imidotriphosphate (Mant-GMP-PNP) (Richter et al., 1995; Scheidig et al., 1995). Given that Mant nucleotides are environment sensitive, their fluorescence increases upon binding to protein and is therefore a direct measurement of nucleotide exchange. As expected, untransfected cells, or cells transfected with the matrix CFP control protein, bind a constant level of Mant-GMP-PNP due to the endogenous GTPases present in the extracts. All samples were normalized to the total cellular protein in the experiment and, for transfected cells, to the signal from the CFP fusion proteins to ensure equal expression of exogenous protein within the experiment. Interestingly, overexpression of Mfn2CFP did not significantly alter the basal amount of nucleotide binding in the extracts (Figure15). Rab5 was also transfected in order to demonstrate that the assay is sensitive enough to detect increased nucleotide binding over the endogenous GTPases within the cell extracts. Overexpression of Rab5 indeed demonstrates a ~4 fold increase in Mant GMP-PNP binding within the first 10 minutes after incubation at 37°C(Figure 15). This signal is specific since addition of unlabeled GTP competes for the binding. Importantly, although transfection of Mfn2CFP had no effect on basal nucleotide binding in this assay, transfection of $Mfn2_{RasG12V}$CFP clearly demonstrated a significant increase in nucleotide binding (Figure 15). These data suggest that, relative to Rab5, wild type Mfn2 does not actively exchange nucleotide under steady state conditions. Given that any GTP bound to Mfn2 would eventually become hydrolysed to GDP, and given the low

Figure 15: Mfn2 has very low intrinsic rates of nucleotide exchange that are increased in the $Mfn2_{RasG12V}$ mutant:
Mant GMP-PNP binding of cell extracts either untransfected (Utf), or transfected with pOCT-CFP (negative control) Mfn2CFP, $Mfn2_{RasG12V}$CFP or Rab5CFP (positive control). Incubations performed at 37°C for 1 and 10 minutes were analyzed in the fluorimeter (see Materials and Methods). Competition with unlabelled GTP was performed for the 10 minute time point only, as indicated. All values obtained were normalized for total protein concentration and for expression levels of CFP tagged proteins and expressed as fluorescence arbitrary units (AU). These results are representative of 4 independent experiments.

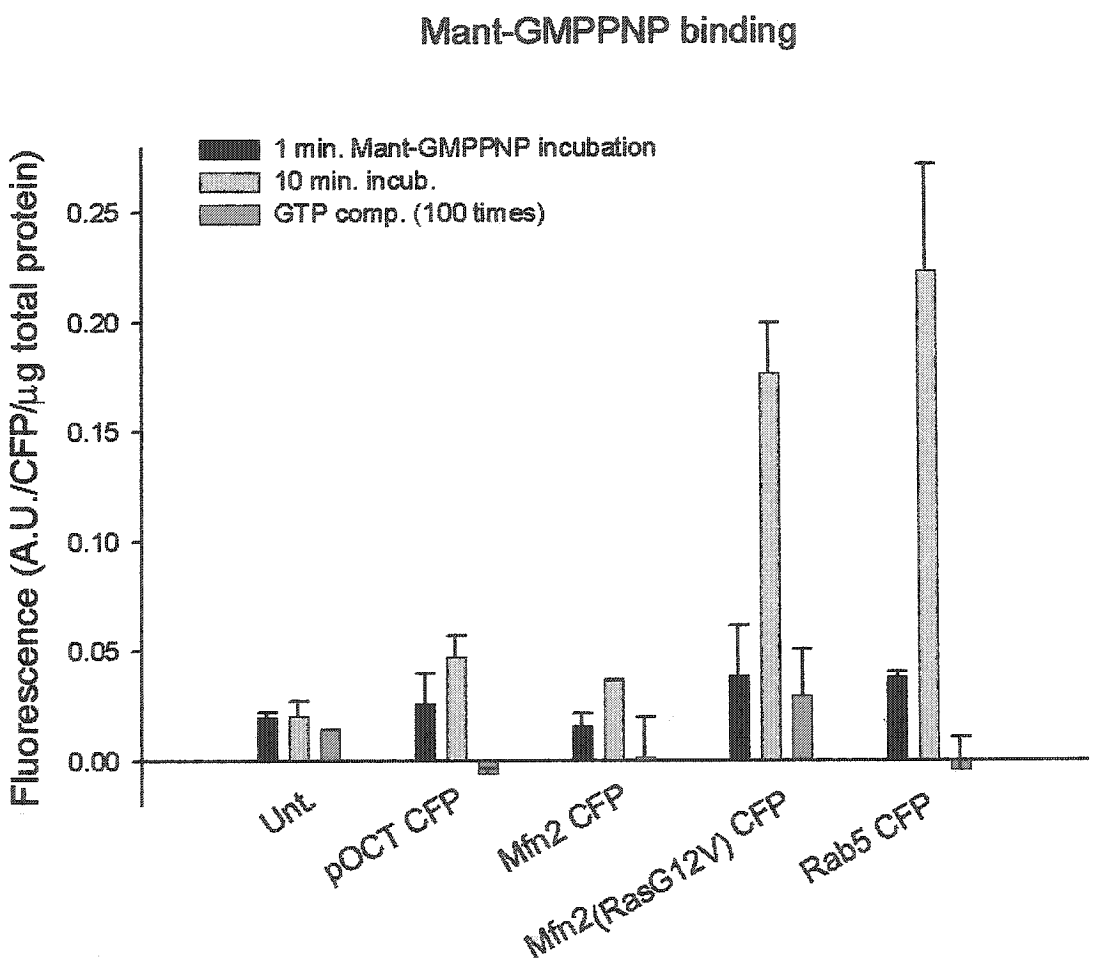
Mant-GMPPNP binding
1 min. Mant-GMPPNP incubation
10 min. incub.
GTP comp. (100 times)
Fluorescence (A.U./CFP/μg total protein)
0.25
0.20
0.15
0.10
0.05
0.00
Unt
pOCT CFP
Mfn2 CFP
Mfn2(RasG12V) CFP
Rab5 CFP

exchange rates we observe, it is assumed that Mfn2 would therefore primarily be in the GDP bound state in the cell. In contrast, since the cytosolic GTP concentration is greater than GDP and Mfn2RasG12V protein has increased rates of exchange, our results indicate that much of the $Mfn2_{RasG12V}$ protein would be in the GTP bound form. Therefore, we have developed a molecular tool to investigate the functional consequences of increasing the GTP bound Mfn2 in transfected cells.

3.2 (c) Morphological consequences of over expressing Mfn2RasG12V

To examine the morphological consequences of overexpressing this mutant, Cos 7 cells were transfected with wild type Mfn2CFP, $Mfn2_{RasG12V}$CFP as well as $Mfn2_{(430-757)}$CFP, which completely lacks the amino terminal GTP binding region and is therefore GTPase deficient. The truncated mutant $Mfn2_{(430-757)}$CFP, is correctly targeted to the mitochondria through the C-terminal signal anchor sequence (Figure 16A), and allows one to test if there is any requirement for the GTPase domain in the function of Mfn2. Examination of Mfn2 expression in transfected cells revealed a very specific localization of the CFP fusion protein to clearly observable spots (or puncta) distributed over the clustered mitochondrial mass (see arrowheads in Figure 16A). In contrast, the CFP tagged $Mfn2_{RasG12V}$ protein no longer appeared in a punctate pattern of expression on the mitochondria, but was instead evenly distributed over the surface of the mitochondria. By 24 hours post transfection, the mitochondria in cells expressing either Mfn2 or $Mfn2_{RasG12V}$ formed collapsed clusters in 95-100% of cells, with the only significant morphological difference being the disappearance of the punctate localization of the transfected $Mfn2_{RasG12V}$ protein (Figure 16A). When the GTPase domain is removed in the $Mfn2_{(430-757)}$CFP protein, within early time points after transfection (8-16 hours) it

was observed that the mitochondria are fragmented and scattered throughout the cell, consistent with a complete block in fusion (Figure 16A). Again, at higher levels of expression, these fragmented mitochondria also collapse and become tethered within clusters, as previously observed for this construct (Rojo et al., 2002 ; Santel and Fuller, 2001). In Figure 16B, line scans were plotted to quantify the arbitrary fluorescent units as a function of pixel distance of a line drawn across the mitochondrial clusters. In the case of the wild type Mfn2 and $Mfn2_{(430\text{-}757)}$CFP, the Mfn2 protein profiles show sharp peaks above the matrix marker profile. However, it is clear from these scans that $Mfn2_{RasG12V}$CFP is distributed evenly over the surface since the profiles of both the matrix marker and the CFP construct mirror each other. The next aim was to understand if the clustered mitochondria or the punctate appearance was affected by the microtubule integrity.

3.2 (d) Nocodazole doesn't dusrupt the clusters

Since microtubules modulate the distribution of mitochondria in the cells (Bereiter-Hahn and Voth, 1994), it was important to understand if the clustered mitochondria also required a cytoskeleton for redistribution. In order to test this, nocodazole was used which severely interferes with the dynamics of the cytoskeleton especially the microtubules. Upon treatment of cells with nocodazole, the perinuclear Golgi stacks were disrupted indicating the loss of the microtubule skeleton. Although Golgi dispersal is evident in the nocodazole treated cells, the mitochondria remain clustered (see figure 17) in all the cells transfected with Mfn2 constructs. This suggests that the Mfn2 protein puncta are not maintained at sites of microtubule contacts, and it also suggests that the mitochondria are directly tethered or fused rather than a clustering

Figure 16: Mfn2 resides in a punctate pattern on mitochondria, which is altered with the Mfn2RV12 mutation.

(A) Cos7 cells co-transfected with pOCT-YFP and the constructs indicated in the side panel. Images were taken from live cells 16 hours after transfection using the 100X objective and a dual pass filter for CFP/YFP (Till Photonics, GmbH). Arrows highlight the Mfn2 puncta along the mitochondrial tubules. In the overlay, the matrix YFP marker is shown in red and Mitofusin2-CFP in green. Scale bars are 1 μm.

(B) Cos7 cells were transiently co-transfected with Mfn2-CFP constructs and pOCT-YFP. Three line scans of total fluorescent signal per pixel are plotted for each Mfn2 construct using the TillVisION software and exported as .tiff files. Red scans are the matrix YFP fluorescent signal, and green scans indicate the CFP channel. 67 pixels = 1 micron. Scans are representative of >20 cells for each condition.

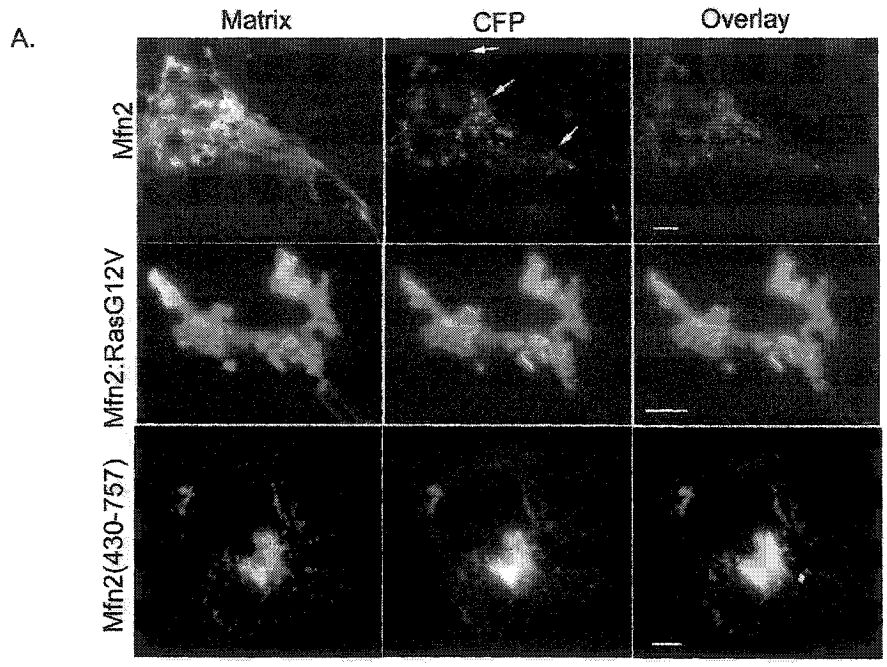
A.
Matrix
CFP
Overlay
Mfn2
Mfn2:RasG12V
Mfn2(430-757)

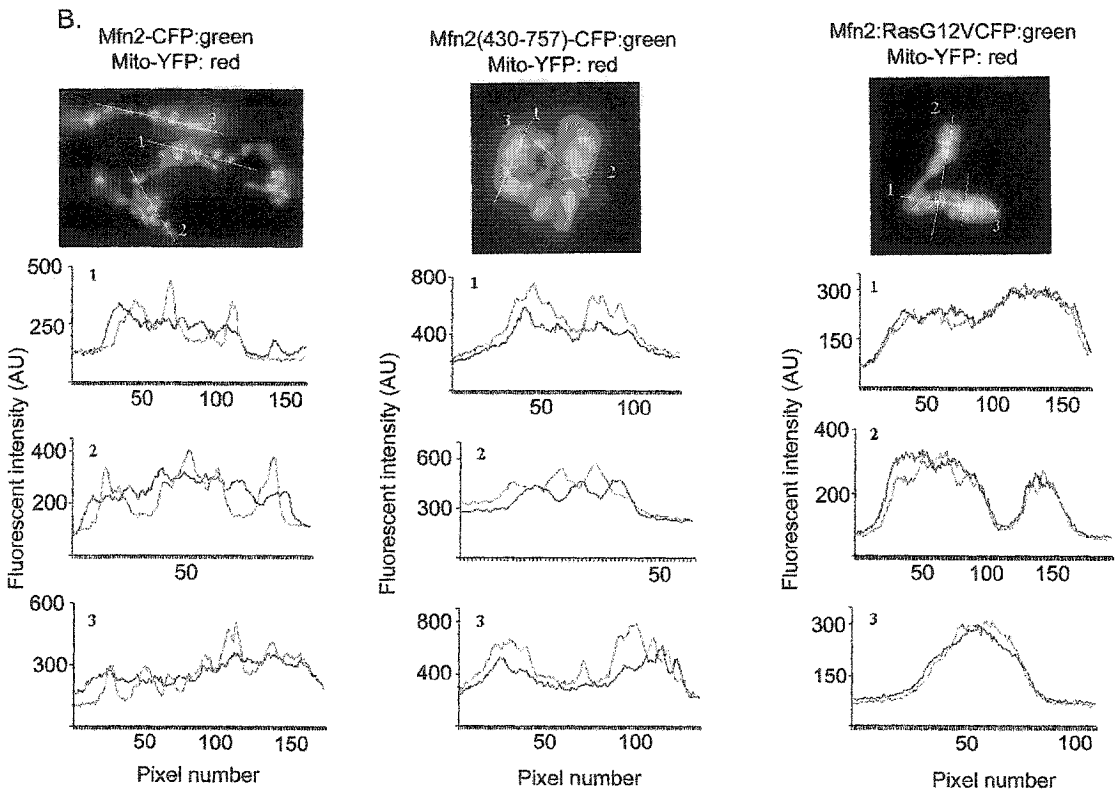
B.
Mfn2-CFP:green
Mito-YFP: red
Mfn2(430-757)-CFP:green
Mito-YFP: red
Mfn2:RasG12VCFP:green
Mito-YFP: red
Fluorescent intensity (AU)
Pixel number

Figure 17: Nocodazole doesn't disrupt the clusters:
In panel (a), shown in red is the mitochondria (labelled with Mitofluor red) and shown in blue is Golgi (Cos 7 cells transfected with Galatosyltransferase:YFP to label the golgi) without nocodazole as a control. It is evident that golgi are tightly packed in the absence of nocodozole. In panels B,C,and D, Cos 7 cells transfected with Mfn2(shown in green), Mfn2RasG12V(green) and Mfn2(430-757) (green) are shown respectively. As can be seen, neither the punctate appearance nor the clustered appearance of the mitochondria is affected in presence of nocodazole but the golgi dispersal is evident. Arrowheads are pointed towards the puncta. In the overlay representations, Golgi is shown blue, mitochondrial matrix is in red and CFP-Mitofusin2 protein is in green.

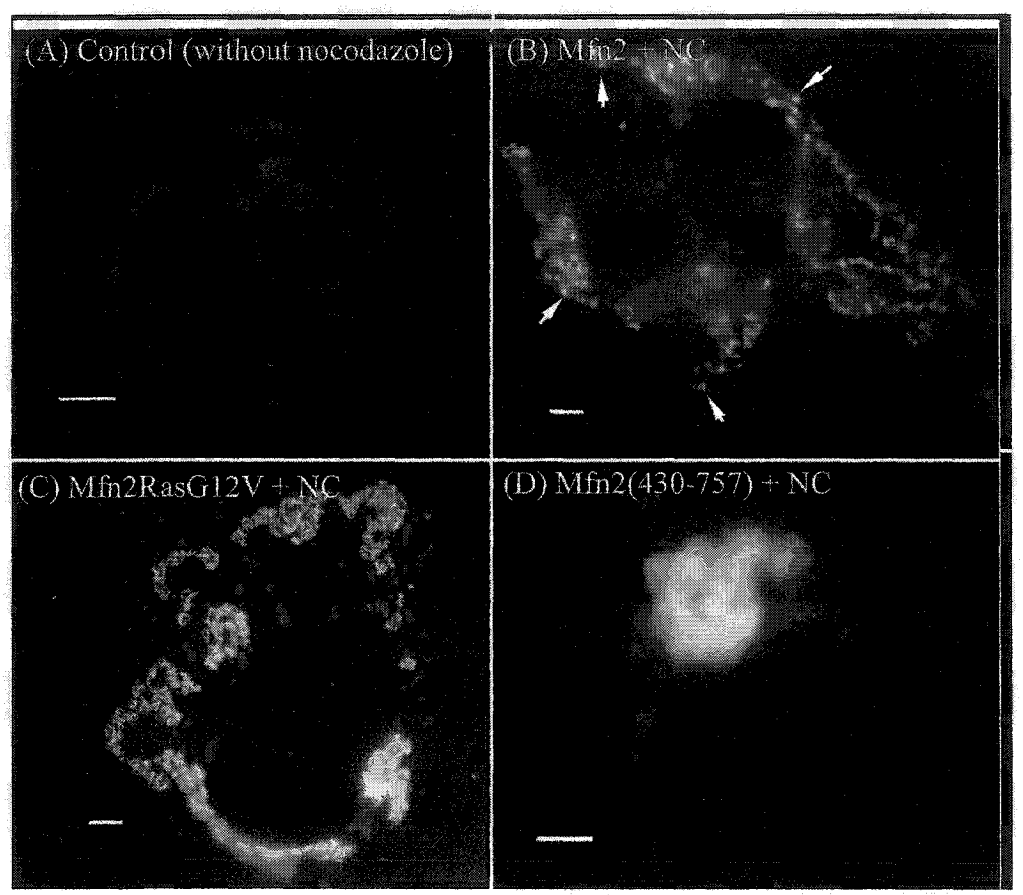
(A) Control (without nocodazole)
(B) Mfn2 + NC
(C) Mfn2RasG12V + NC
(D) Mfn2(430-757) + NC

of organelles due to an effect on motility.

3.2 (e) PEG induced cell fusion demonstrates that activated Mfn2 stimulates mitochondrial fusion.

Although the fluorescent images suggested that $Mfn2_{(RasG12V)}$CFP stimulated mitochondrial fusion and rearrangement of the protein puncta, it is not a demonstration of matrix content mixing. To directly test this, a previously used assay was employed that induces whole cell fusion of cells transfected with different matrix marker proteins (Legros et al., 2002). Given that the mitochondrial clusters observed in cells expressing $Mfn2_{(RasG12V)}$CFP are immobile, we chose to fuse these cells with wild type cells expressing a mitochondrial GFP marker, in order that the wild type mitochondria would be able to move towards the induced mitochondrial clusters. Cells transfected with pOCT:GFP were fused with those transfected with either pOCT:DsRed2 alone or with cells cotransfected with pOCT:DsRed2 and Mfn2CFP or pOCT:DsRed2 and $Mfn2_{(RasG12V)}$CFP. Fused cells were imaged in a time course from 30 minutes post-PEG fusion until 8 hrs post-PEG fusion. In all experiments cyclohexamide was added 2 hours prior to PEG fusion in order to inhibit new synthesis of the marker proteins, and was maintained throughout the experiment. As previously reported (Legros, 2002), mitochondria from wild type cells fused completely within 8-12 hours (Figure 18). Mitochondria from cells expressing Mfn2CFP also fused within a similar time course in most cases (Figure 18, n=20). Approximately 20% (4 cells out of 20) of the fused cells expressing Mfn2CFP showed that mitochondrial fusion reached complete content mixing

Figure 18: PEG fusion assay:

COS7 cells transfected with pOCT-GFP and pOCT-DdRed2 (top panel) were seeded together for 12 hours and 50% PEG 5000 was added for 60 seconds following a 2 hour pre-incubation with cyclohexamide. Images of both fluorophores were taken from live cells after 1 hour, 4 hours and 8 hours. The overlay of the pOCT-GFP (green) and pOCT-DsRed (red) is shown for each time point. The time course from COS7 cells transfected with pOCT-GFP fused to cells co-transfected with pOCT-DsRed2 and Mfn2: CFP is shown in the middle panel, and the fusion of pOCT-GFP transfected cells with cells co-transfected with pOCT-DsRed and $Mfn2_{(RasG12V)}$:CFP is shown in the bottom panel.

Mfn2RasG12V
Mfn2
Untransfected
1 hr
4 hrs
8 hrs

within 2-5 hours. Most surprising was the increased rate of fusion in cells expressing $Mfn2_{(RasG12V)}$CFP, whose matrix targeted GFP and DsRed contents were completely mixed within 30 minutes to 1 hour after the addition of PEG in >90%(18 cells out of 20) of the observed cell fusions (Figure 18, n=20).

3.2 (f) Clustered mitochondria are interconnected by novel tubular membrane elements.

In order to understand the differences between the fused phenotypes of the wild type Mfn2 and Mfn2RasG12V at the ultrastructural level, Cos7 cells were transfected with each of the constructs, fixed the cells and processed the samples for imaging by electron microscopy. Cells transfected with Mfn2CFP showed very unique mitochondrial morphology. Most striking is the appearance of interconnected tubules running throughout the mitochondrial clusters. This membrane material often appears to be holding a number of mitochondria together in bundles (Figure 19). The cristae structure of mitochondria expressing Mfn2 appears normal, although many mitochondria appeared to have fewer cristae than in untransfected cells. It was also difficult to distinguish specific contact sites within these membranous regions, so the interpretation of these structures is challenging. Cells expressing $Mfn2_{(430-757)}$CFP showed clearly fragmented rounded mitochondria with normal cristae and no extra tubular interconnecting membranes. Mitochondria of cells expressing $Mfn2_{(430-757)}$CFP were also found in large clusters (see low magnification image in Figure 19), however it was clear that the mitochondria within the clusters are not interconnected in any way nor is there any excess membrane material within the clusters. Interestingly, although the fluorescent

Figure 19: Ultrastructural Analysis reveals interconnected mitochondrial tubules upon overexpression of Mfn2 and $Mfn2_{RasG12V}$.
Representative images taken at 40,000 - 50,000X magnification are shown from mitochondrial clusters in three different cells expressing each of Mfn2CFP, $Mfn2_{(430-757)}$CFP and $Mfn2_{RasG12V}$CFP. Mitochondria from untransfected cells are also shown at a slightly lower magnification (12,000X) for comparison. Within the clusters of cells transfected with Mfn2CFP and Mfn2RasG12VCFP, the mitochondria are extremely closely opposed and are interconnected by multiple membrane elements that often appear to be continuous and indistinguishable from the mitochondrial outer membrane. Mitochondria from cells transfected with Mfn2(430-757)CFP are not as closely opposed and no additional membrane material is present within the clusters.

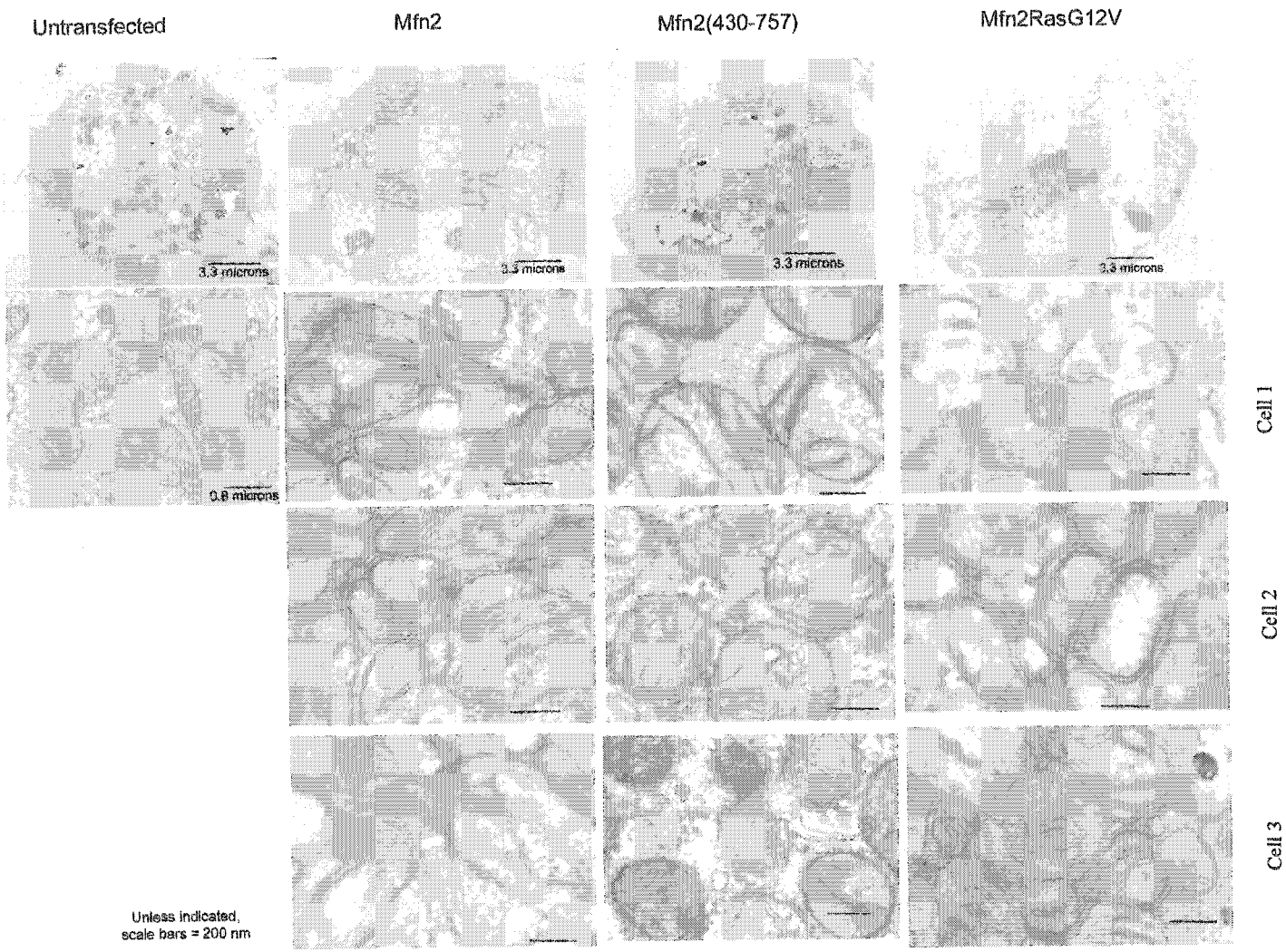
Untransfected
Mfn2
Mfn2(430-757)
Mfn2RasG12V
3.3 microns
0.8 microns
Cell 1
Cell 2
Cell 3
Unless indicated,
scale bars = 200 nm

profiles of Mfn2 localization within the mitochondrial clusters are different between Mfn2 and $Mfn2_{RasG12V}$, the ultrastructural analysis of the two transfections did not reveal any striking differences. The mitochondria in cells expressing $Mfn2_{RasG12V}$CFP form similarly large clusters that also contain an incredible proliferation of tubular membranes. The number of clearly defined cristae in mitochondria of cells expressing $Mfn2_{RasG12V}$CFP was also reduced and many mitochondria had totally empty matrix compartments suggesting a total loss in cristae but the size of the mitochondria appeared to be larger than the untransfected cells. These data demonstrate that at least the outer membranes of the mitochondria within the clusters of both Mfn2CFP and $Mfn2_{RasG12V}$CFP have become interconnected and fused, and that this phenomenon is completely dependent on the presence of the GTPase domain of Mfn2.

3.2 (g) Interconnected mitochondria are protected from free radical damage.

Given the highly fused nature of the Mfn2RasG12V transfected cells, the next aim was to investigate the functional consequences of increased interconnectivity. Therefore, an assay which was previously used to determine the level of connectivity within the mitochondrial reticulum in live cells which also exposes the mitochondria to damaging free radicals (Collins et al., 2002 ; De Giorgi et al., 2000; Huser and Blatter, 1999) was employed.. The $\Delta\Psi$ (mitochondrial electrochemical potential) sensitive dye tetramethyl rhodamine ester (TMRE) becomes photoactivated upon exposure to light and produces free radicals within the matrix of the mitochondria. With the increasing accumulation of free radicals, the permeability transition pore opens and protons become equilibrated across the inner membrane (De Giorgi et al., 2000; Huser and Blatter, 1999).

With this loss in $\Delta\Psi$, TMRE is redistributed within the cell, a process that can be observed using time-lapse video microscopy. The mitochondria then regain $\Delta\Psi$ and accumulate more dye, and in time lapse, appear to "flicker" until they become terminally depolarized. The ability of the mitochondria to resist activated TMRE induced flickering is therefore an indication of the metabolic protection conferred on the organelle. One hundred images were collected over 2.5 minutes by exciting TMRE at 549 nm for 500 msec, followed by a 1000 msec delay. Untransfected cells incubated with 50 nM TMRE clearly show a striking and immediate loss in TMRE of individual mitochondrion followed by re-entry of TMRE, until the organelle is terminally depolarized (Figure 20, top panel and supplemental videos). It was also observed that most mitochondria within a single cell flicker at different times (compare each area of interest (AOI) in Untransfected panel of Figure 20), consistent with the idea that the threshold for free radical accumulation in individual matrices is unique. As expected, TMRE loading of cells transfected with $Mfn2_{(430\text{-}757)}$CFP at all levels of expression exhibited highly distinct patterns of TMRE uptake and release cycles, consistent with the previous data indicating that they are not fused, but fragmented into small, spherical mitochondria (Figure 20, compare TMRE profiles of AOIs 1-6 in $Mfn2_{(430\text{-}757)}$ panel). Furthermore, even after longer times of expression, these small mitochondria cluster together, but TMRE flickering remains asynchronous, demonstrating that they can never fuse. Therefore, in the absence of the GTPase domain, the remaining coiled coil regions of Mfn2 are dominant interfering and mitochondrial fusion is completely blocked.

As a positive control for interconnected mitochondria, Cos 7 cells were transfected with the dominant interfering mutant of the mitochondrial dynamin protein,

Figure 20: TMRE flickering indicates degree of matrix content mixing within Mfn2 induced mitochondrial clusters.

COS7 cells transiently transfected with Mfn2CFP, $Mfn2_{RasG12V}CFP$ or $Mfn2_{(430-757)}CFP$ were incubated for 12 hours before incubation with 50 nM TMRE in complete DMEM medium at 37 degrees. After 15 minutes of loading, 100 images were taken of both transfected and untransfected cells by exciting at 549 nm for 500 msec, followed by a 1 second delay. Each transfection condition is indicated along the left side, and the TMRE panel shows initial TMRE loading into the mitochondria. The CFP panels show the localization of the transfected CFP tagged proteins for the same area. Arrows highlight the Mfn2 puncta present along the tubules of transfected cells. Areas corresponding to individual mitochondria were selected (areas of interest, AOI) and cropped as shown in the boxes of the TMRE panel, and the total fluorescence within the areas was plotted after subtracting the background fluorescence. Values from each of 50 frames were plotted, as indicated in the graph. This gives an indication of the frame-by-frame variation in TMRE release and reloading from distinct areas up to 3 μm apart. The accompanying videos of these experiments are included in the supplementary online materials, Video2 through Video6. Scale bars are 1 μm.

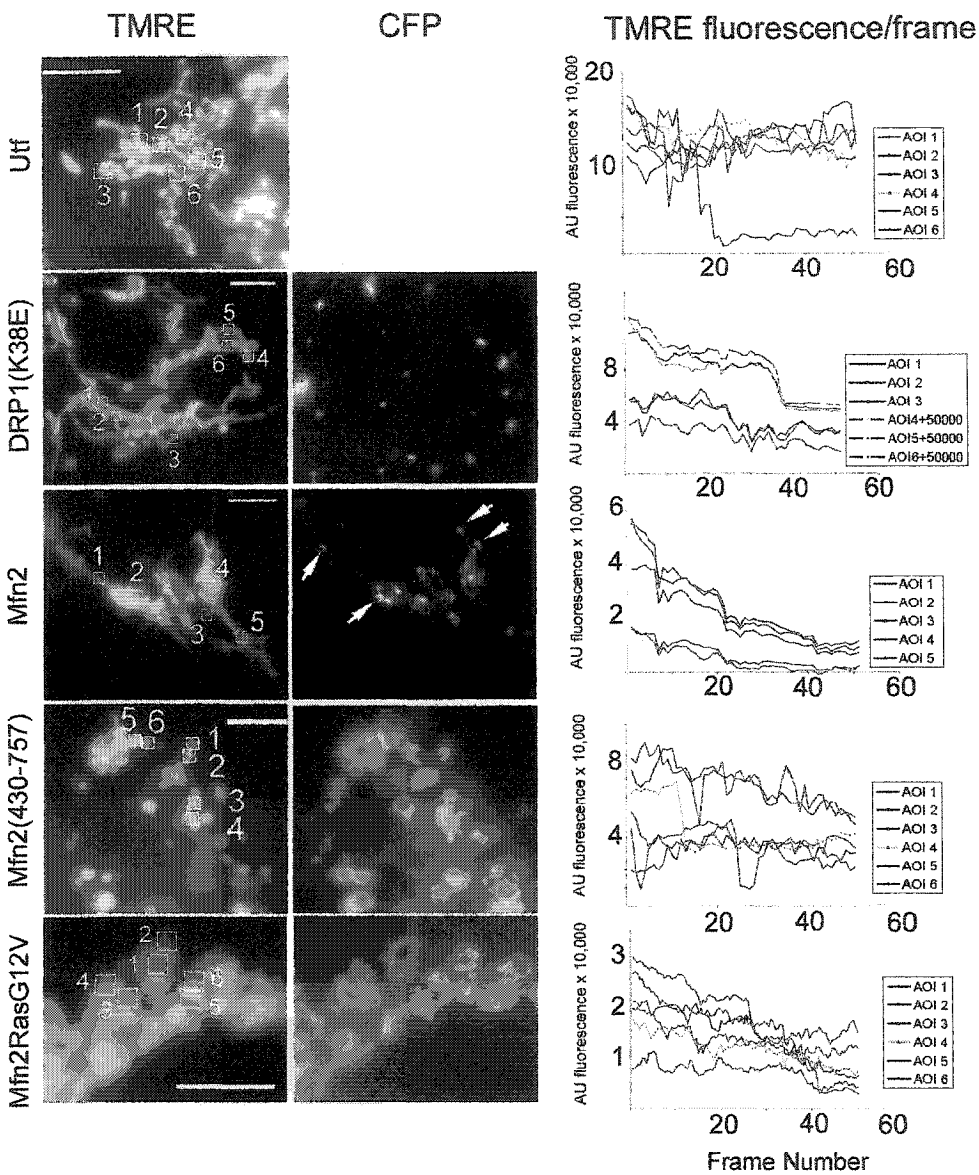
TMRE
CFP
TMRE fluorescence/frame
Utf
DRP1(K38E)
Mfn2
Mfn2(430-757)
Mfn2RasG12V
AU fluorescence x 10,000
Frame Number
AOI 1
AOI 2
AOI 3
AOI 4
AOI 5
AOI 6
AOI4+50000
AOI5+50000
AOI6+50000

DRP1(K38E). DRP1K38E inhibits mitochondrial fission, however since fusion continues, the result is a continuous mitochondrial reticulum after 24-48 hours of DRP1K38E expression (Griparic and Vander Bliek, 2001; Labrousse et al., 1999; Smirnova et al., 2001). As can be seen in Figure 20, the flickering traces of different AOIs within the mitochondrial reticulum in cells expressing DRP1(K38E)CFP was also synchronous, consistent with a block in mitochondrial fission. It is interesting to note that the mitochondria are not necessarily fused into a single reticulum, but often fuse into a few distinct networks. In the DRP1(K38E)CFP transfection, for example, two separate mitochondrial networks are shown within one cell (compare AOIs 1-3 with AOIs 4-6, Figure 20, DRP1 panel). What is evident from the traces of individual AOIs is that the quantal release of TMRE from each frame is dramatically less that that of the untransfected or the fragmented cells transfected with Mfn2(430-757)CFP). Consistent with the fact that Mfn2 can fuse mitochondria, these entire bundles flicker together in a highly synchronous manner, unlike the individual mitochondria of untransfected cells (Figure 20, compare AOIs in Mfn2 TMRE profile). The quantal release of TMRE from each AOI trace was also reduced relative to untransfected and Mfn2(430-757)CFP transfected cells.

Suprisingly, the fused reticulum of mitochondria in cells expressing $Mfn2_{RasG12V}$CFP flickered in a highly asynchronous manner, with a much reduced quantal loss of TMRE from each AOI (compare TMRE profiles of AOIs 1-6 of $Mfn2_{RasG12V}$ panel, Figure20). Since TMRE is lost at different times from the individual AOIs within the fused cluster, by the end of the time series, the remaining tubular elements highlight the outline of the original cluster and correlates with the localization of the CFP tagged protein. The

quantification of the total TMRE dye remaining in cells transfected with Mfn2RasG12V compared to control cells shows that dye remaining was increased from 15% in untransfected cells to 40% in cells transfected with Mfn2RasG12V. This indicated that the response of Mfn2RasG12V to free radical induced damage was very low compared to the controls. In untransfected cells there was no TMRE dye remaining after 60 frames, in cells transfected with Mfn2, the dye remained even after 80 frames and in cells transfected with Mfn2(430-757), there was no dye remaining after 40 frames suggesting that the RasG12V transfected cells have interfered with the free radical induced damage. The total numbers of cells counted were 8 for each. (Figure 21)

3.2 (h) Supplemental Videos are available on the CD (Page 99)

Figure14 Video1: This video shows a cropped section of a Cos7 cell transfected with pOCT-YFP matrix marker protein, as shown in Figure 14. All the frames were taken 2 seconds apart for an exposure time of 300 msec each and are shown over a 400 second period.

Figure 20 Video1: This video shows a cropped section of an untransfected Cos7 cell loaded with 50 nM TMRE, as shown in the top panel of Figure 20. 100 images were taken 1000 msec apart and were exposed for 500 msec each. The frames are played back over a 3 second period.

Figure 20 Video2: This video shows a cropped section of a Cos7 cell transfected with DRP(K38E)CFP and loaded with 50 nM TMRE, as shown in the second panel of Figure

20. 100 images were taken 1000 msec apart and were exposed for 500 msec each. The frames are played back over a 3 second period.

Figure 20 Video3: This video shows a cropped section of a Cos7 cell transfected with Mfn2CFP and loaded with 50 nM TMRE, as shown in the third panel of Figure 20. 100 images were taken 1000 msec apart and were exposed for 500 msec each. The frames are played back over a 3 second period.

Figure 20 Video4: This video shows a cropped section of a Cos7 cell transfected with $Mfn2_{(430\text{-}757)}$CFP and loaded with 50 nM TMRE, as shown in the fourth panel of Figure 20. 100 images were taken 1000 msec apart and were exposed for 500 msec each. The frames are played back over a 3 second period.

Figure 20 Video5: This video shows a cropped section of a Cos7 cell transfected with $Mfn2_{RasG12V}$CFP and loaded with 50 nM TMRE, as shown in the fifth panel of Figure 20. 100 images were taken 1000 msec apart and were exposed for 500 msec each. The frames are played back over a 3 second period.

Figure 21: TMRE flickering assay:
The TMRE dye remaining in cells transfected with different constructs was quantified. In untransfected cells, there was no dye remaining after 40 frames. In cells transfected with Mfn2 , there was no increase in the dye remaining in the cells but 20% of the dye remained in the cells until 100 frames. In cells transfected with Mfn2RasG12V, there was an increase in the dye remaining in the cells from 20 to 40%. In cells transfected with Mfn2 (430-757), the % of dye remaining in the cells decreased from 65% to 25%.

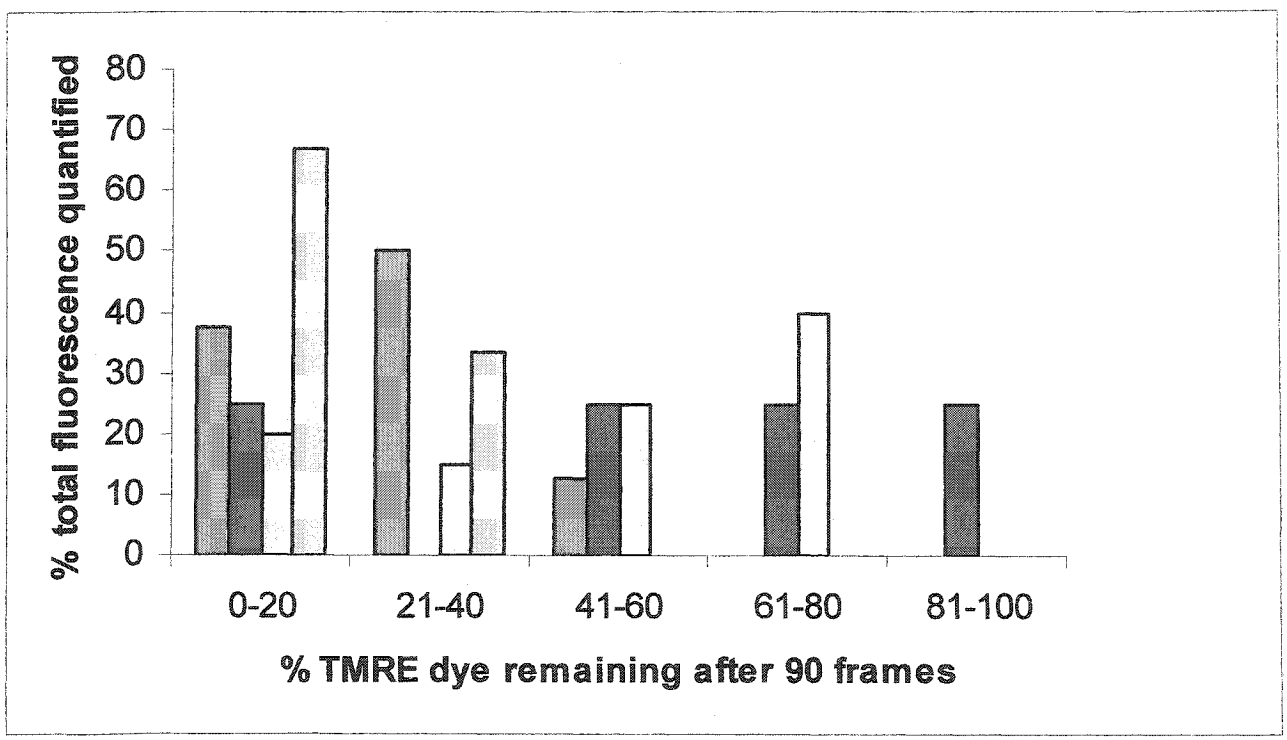

Untransfected

Mfn2

Mfn2RasG12V

Mfn2 (430-757)

4. Discussion

4.1 Two-Hybrid screens are useful only for highly soluble proteins.

Mfn2 may function as a regulatory GTPase that governs mitochondrial tethering, similar to the family of small Rab GTPases (Zerial, 1993; Novick, 1993), where the GTPase domain interacts with the effector molecules and mediates the downstream functions. However, since Mfn2 is a novel class of GTPase, it is also possible that it participates enzymatically in the assembly of a pore through which lipid bilayers mix resulting in fusion of the outer membranes. One of the ways to distinguish between these possibilities is to identify other proteins that participate in this pathway, in particular, those that functionally interact with Mfn2. The predicted GTPase domain of Mfn2 was used as a bait to search for proteins expressed by Hela cDNA library in a yeast two-hybrid screen. The positive clones isolated in this screen were considered to be false due to the following reasons. The first was that the time it took for the blue colonies to appear in the colony lift assay for the positive clones was very long (3 hrs for homeobox gene and more than 4 hrs for the rest of the clones) in comparison to the positive control which was the interaction between Rab5Q79L and Rabaptin5 (20 minutes). The β-galactosidase units in the liquid assay were very low in comparison to the positive control (see figure 11). During the screen, it was realized with biochemical studies that the GTPase domain of Mfn2 was extremely insoluble, which is likely another reason for the lack of success in this screen. This insolubility may result in low targeting of LexA-Mfn2(1-560) to the nucleus within the yeast which is a very important step for a successful yeast two hybrid screen. Mfn2 has no predicted transmembrane domains and the insolubility suggests that this protein may exist in a multiprotein complex and therefore is not soluble when expressed in isolation. A second possibility could be that the protein is in the GDP bound

and largely in the inactive form. For example, Rab GTPases bind to the effectors only when they are in the GTP form, which is the active form. Other possibilities, which cannot be excluded, are incorrect folding of the bait, because correct folding and ability to exist as a stable protein inside the yeast cells is very important for a successful two-hybrid screen. Another important aspect for a two-hybrid screen to be successful is the transformation efficiency, which has to be high enough to screen most of the library.

4.2. Affinity chromatography identified a number of Mfn2 interacting proteins

Although the GTPase region is insoluble when expressed recombinantly, Mfn2 also has a soluble coiled coil domain at the carboxy terminal region which is exposed to the cytosol (Rojo, 2002). This soluble cytosolic carboxy terminal region is predicted to form a coiled coil similar to the SNARE proteins, which are essential for vesicular fusion events (Weimbs et al., 1997; Sollner, 2002; Rothman and Sollner, 1997). When this region is transfected alone, it resulted in inhibition of fusion and dramatic clustering of mitochondria around the nucleus of the cell and the protein accumulates at very discreet sites within the mitochondrial clusters, which appear to be interface between docked mitochondria (See section 3.2(c)). This suggested that the C-terminal coiled coil region may be interacting directly with other proteins involved in the fusion pathway. In order to test this, we made use of the affinity chromatography using recombinant Mitofusin2 (710-757) as bait and retrieved at least 7 specific proteins from mitochondrial lysates. The identities of the bands are shown in Table3. The conditions used for this purification suggest that the complex is completely stable under high salt and detergent conditions reminiscent of the TRAPP (Transport protein particle) complex (Sacher et al., 1998)

which is present on the Cis-golgi and mediates vesicle fusion and Exocyst (TerBush et al., 1996) which is a large complex of proteins functioning as a tethering complex to direct secretory vesicles to specific sites on the plasma membrane. Given these results, the affinity column approach was found to be more successful than the hybrid screen and in the future, another approach to find the interacting proteins would be to perform immunoprecipitations using antibodies. Finally, antibodies against Mfn2 are prepared which will allow future members to follow the endogenous Mfn2 complex.

In conclusion, regarding the methods for identifying the interacting proteins, given my experience, each method has advantages and disadvantages, depending on the nature of the interaction that is being searched for. In our case, the soluble coiled coil region was the most promising and the future work in the lab will focus on identifying the bands and studying the interactions.

4.3. Mfn2 is a powerful regulatory GTPase

The results obtained from the morphological and biochemical assays provide the first insights into the role of the GTPase activity of Mfn2 in stimulating fusion. Overexpression of Mfn2 results in a network of mitochondria, which according to electron microscopy, PEG fusion assay and TMRE flickering experiments, are highly interconnected and fused. This is consistent with the large body of data indicating that fission and fusion are in dynamic equilibrium, in that the increase in cellular levels of functional Mfn2 results in a shift of this balance towards mitochondrial fusion. Previous published data has provided evidence that upon high levels of expression of Mfn2, the mitochondria collapse into perinuclear clusters that did not appear fused (Rojo et al., 2002; Santel and Fuller, 2001). By employing high-resolution fluorescence assays

combined with electron microscopy, these clusters were resolved further and demonstrate that expression of Mfn2 instead stimulates mitochondrial fusion. The stimulation of mitochondrial fusion granted by the overexpression of Mfn2 is absolutely dependent on the presence of the GTPase domain since the mitochondrial morphology in cells expressing $Mfn2_{(430\text{-}757)}$CFP are tethered and fragmented but neither their inner or outer membranes have fused. Through the creation of a mutation that increases the levels of GTP bound Mfn2, our fluorescent images, PEG fusion assay, combined with ultrastructural analysis by electron microscopy have demonstrated that the stimulated activation of Mfn2 to the GTP bound state highly stimulates mitochondrial fusion. The proliferation of interconnected membranes observed by electron microscopy confirms that mitochondrial membrane fusion events are highly stimulated and sheds new light on the plasticity of the mitochondria. Finally, we have observed by fluorescence imaging that Mfn2CFP is localized to distinct subdomains along mitochondrial tubules, which are also lost upon increased binding to GTP.

Given these data, what is the function of the nucleotide switch in Mfn2? Interestingly, the Mant GMP-PNP binding experiments suggest that under steady state conditions, Mfn2 resides in specific sites on the mitochondrial membrane primarily in the GDP bound, inactive form with extremely low rates of nucleotide exchange (Figure 15). This novel finding suggests that the activation of Mfn2 to the GTP bound state must occur at highly select moments during the docking and fusion events, and that Mfn2 does not have a significant "futile cycle" of nucleotide exchange and hydrolysis (Rybin et al., 1996). In contrast, increased activation of Mfn2 using the $Mfn2_{RasG12V}$CFP construct results in the striking loss of the Mfn2CFP fluorescent puncta, demonstrating that the

assembly and disassembly of these sites is nucleotide dependent. It is considered that the punctate appearance of Mfn2 is significant and is consistent with the biochemical studies in yeast demonstrating that Fzo1p is part of a larger, 800 kDa complex localized to contact sites between the outer and inner membranes (Fritz et al., 2001; Rapaport et al., 1998; Reichert and Neupert, 2002). Importantly, in other membrane transport systems, similar large tethering/fusion complexes are known to play essential roles in membrane docking and fusion events. Docking and fusion complexes like the Exocyst, HOPS (homotypic fusion and vacuole protein sorting), and TRAPP complexes can be up to 60 Svedbergs in size, are often visible as discreet sites on the membrane and their dynamics are also regulated by GTPase switches (Guo et al., 1999; Jones et al., 2000 ; McBride et al., 1999; Price et al., 2000; Sacher et al., 1998; TerBush et al., 1996; Wang et al., 2000). Therefore, it is proposed that the punctate localization of Mfn2CFP reflects stable mitochondrial docking sites competent to fuse the outer and inner membranes concomitantly. Upon increased activation of Mfn2 to the GTP bound form ($Mfn2_{RasG12V}$), these punctate complexes are lost, and fusion between both outer and inner membrane fuse in an uncontrolled manner. The exaggeration of tubular membrane connections running through the mitochondrial clusters apparent in EM micrographs of both Mfn2 and $Mfn2_{RasG12V}$CFP transfected cells suggests that outer membrane fusion has been profoundly stimulated. This data provides two important findings, first it demonstrates that Mfn2 is a highly potent stimulator of fusion and it is therefore imperative that it remain in the GDP bound state in order that mitochondria fuse only upon very specific triggers. Second, given that both membranes are able to fuse upon expression of only Mfn2, it suggests that the fusion between these membranes is highly

co-ordinated. This is the first demonstration that activated Mfn2 behaves like other regulatory GTPases, such as Rab proteins. Expression of dominant active forms of Rab5, for example, leads to uncontrolled fusion of the early endosomal system resulting in large, vacuolar endosomes containing all the markers of the Rab5 positive early endosome. Similarly, expression of the dominant active form of Mfn2 results in complete fusion within 30 minutes of PEG fusion, which is ~16 times faster than wild type cells. The importance of this finding in terms of the mechanism of the GTPase is that it suggests a) that GTP hydrolysis is not required for fusion to occur and b) that Mfn2 is a key regulatory protein (i.e.; non-enzymatic) capable of signaling mitochondrial fusion events without overexpression of other proteins. It is likely then, that upon activation, Mfn2 can recruit cytosolic factors that contribute to the fusion event. However, until those factors are identified, it cannot be ruled out that activated Mfn2 can drive fusion directly without the participation of contributing proteins. In addition, it is important to note that Mfn2RasG12V was able to stimulate recruitment and fusion with mitochondria not expressing the activated protein. This lends further evidence to support the idea that other signalling molecules, both mitochondrial and/or cytosolic, have been engaged upon activation of Mfn2.

4.4. The role of fusion in mitochondrial protection against free radicals

The functional consequences of mitochondrial fusion as demonstrated using TMRE flickering experiments suggest that increased interconnectivity of the mitochondrial reticulum, by expressing DRP (K38E), Mfn2 or Mfn2RasG12V, allows a greater protection of the cluster to artificially induced free radical damage. Importantly, the extreme asynchrony of TMRE flickering in Mfn2RV12 expressing cells relative to

DRP(K38E) or Mfn2 transfected cells, suggests that activated Mfn2 is a more potent protector of radical damage than the wild type Mfn2. This leads to the question of how activated Mfn2 is able to provide this protection. Interestingly, the affinity column shown in Figure12 resulted in the identification of an unlikely candidate, catalase, as an interacting partner of Mfn2. Initially, this was considered a potential false positive, or contaminating band since the majority of catalase is localized within peroxisomes where it converts damaging peroxides to water and oxygen. However, upon reading the literature on this subject, it was easy to find many reports that identify catalase immunoreactivity in the cytosol. Catalase was initially localized by immunoelectron microscopy and subcellular fractionation mainly to the peroxisomes but was also found in the cytosolic fractions and in some cell types, also the mitochondria (Radi et al., 1991). Catalase contains a class 1 peroxisomal targeting signal (PTS1), which does not conform perfectly to the consensus and is therefore an inefficient signal sequence (Knott et al., 2000). This observation has led some in the field to suspect that the slow sorting of catalase may have evolved in order to fulfill a functional purpose within the cytosol. For these reasons, an interaction between activated Mfn2 on the mitochondrial surface with cytosolic catalase cannot be neglected. Given that activated Mfn2 renders protection of the mitochondrial reticulum against free radical damage, perhaps the regulated recruitment of catalase is an important part of mitochondrial biology. Further, these data suggest that one of the primary functions of dynamic mitochondrial fusion may be to routinely protect against oxidative damage that results from steady state respiration within the cell. With the experimental systems developed thus far, we have identified a specific function for the GTPase activity of Mfn2. This study demonstrated that Mfn2 is

a potent fusion factor whose nucleotide state regulates the assembly and/or maintenance of discreet sites that define the local fusion sites. Future studies will focus on the identification of other components within the endogenous Mfn2 complex, and to continue investigations into the functional consequences of the fused mitochondrial reticulum.

5. Conclusions and directions for the future:

This investigation addresses the dynamic behaviour of mammalian mitochondria under steady state conditions and has observed that mitochondria fuse with surprising regularity. Given the previous work in Drosophila and yeast genetics, we were able to isolate the human homologue of the GTPase, Fzo1p, responsible for mitochondrial fusion which is now called Mitofusin 2. Mfn2 has two distinctly important regions, the carboxy terminal coiled region and a GTPase domain. When the carboxy terminal coiled region is transfected alone (Section 3.2©), the mitochondria cluster around the nucleus of the cell and the protein accumulates at very discreet sites within the mitochondrial clusters. Results demonstrated in this study suggest that the carboxy terminal coiled region is responsible for the dominant interfering effect meaning that it is interfering with the normal process of mitochondrial fusion and allows the mitochondria just to dock. The results from the affinity column suggest that this coiled coil domain interacts with several other proteins and also that this complex is stable under high salt and detergent conditions.

This study also showed a functional role of GTPase domain of Mitofusin2 in the regulation and activation of mitochondrial fusion in mammalian cells. Previous work demonstrated that the nucleotide binding by Mitofusin2 is important for fusion but did not identify the precise function for the GTP switch mechanism in Mitofusin2. This work has uncovered a novel function for Mfn2 in the stimulation of mitochondrial fusion where the matrix contents are mixed completely and this activity is absolutely dependent upon the GTPase binding domain. In addition, it was observed that Mfn2CFP is localized to discreet sites of intense fluorescence along the mitochondrial tubules, which are lost upon activation of Mfn2. The creation of a dominant active form of Mfn2 results

in highly stimulated fusion and loss of the discreet Mfn2 puncta, suggesting Mfn2 is a regulatory GTPase, which upon increased exchange to the GTP bound form is capable of signalling fusion events to wild type mitochondria. This study also confirmed that the assembly of the puncta are not related to contacts with the microtubules but are tethered directly. The fused mitochondrial reticulum also shows increased protection against free radical damage, demonstrating a novel physiological function for mitochondrial fusion in cellular protection.

A recent study linking metabolism and mitochondrial dynamics suggests that the proteins involved in maintaining the mitochondrial network may be involved in the controlling the energy metabolism in mitochondria. They demonstrate that Mfn2 controls mitochondrial metabolism by observing decreased membrane potential decreased glucose oxidation, reduced proton leak when Mfn2 is repressed (Bach et al., 2003). As described in the results of the TMRE assay to analyse the function of Mfn2, the mitochondria had an ability to resist the free radical induced damage in cells transfected with Mfn2RasG12V. Given that the coiled coil domain of Mitofusin2 is able to recruit catalase to an affinity column, it would suggest that the regulated recruitment of catalase might confer the metabolic protection of the mitochondria. The tools have been developed to study the protection against free radical damage when fusion is stimulated or blocked and this will be useful for the lab to look more into metabolic consequences of mitochondrial fusion in the future.

Future work will undoubtedly uncover the other components interacting with Mfn2 within the puncta. The work described in this thesis will be the springboard for future studies. These studies have determined the next stages that will be taken by the

laboratory to characterize the proteins identified in the affinity column and to continue to search for the GTPase modulating proteins (exchange factors and GTPase activating proteins) that regulate the nucleotide state of mitofusin2. Finally, by taking these mechanistic approaches, this work will eventually lead to the identification of the endogenous triggers that activate Mfn2 to drive mitochondrial fusion under normal cellular conditions. Future work in the lab will continue to investigate the role of cytosolic catalase as an effector of Mfn2 and the relationship between these proteins and the stimulation of mitochondrial fusion events.

6. References

Albert, S., Will, E., and Gallwitz, D. (1999). Identification of the catalytic domains and their functionally critical arginine residues of two yeast GTPase-activating proteins specific for Ypt/Rab transport GTPases. Embo J 18, 5216-25.

Bach, D., Pich, S., Soriano, F. X., Vega, N., Baumgartner, B., Oriola, J., Daugaard, J. R., Lloberas, J., Camps, M., Zierath, J. R., Rabasa-Lhoret, R., Wallberg-Henriksson, H., Laville, M., Palacin, M., Vidal, H., Rivera, F., Brand, M., and Zorzano, A. (2003). Mitofusin-2 determines mitochondrial network architecture and mitochondrial metabolism: a novel regulatory mechanism altered in obesity. J Biol Chem 21, 21.

Bartel, P. L., Chien, C.-T., Sternglanz, R., and Fields, S. (1993). Using the two-hybrid system to detect protein-protein interactions. In Cellular interactions in development: A practical approach, D. A. Hartley, ed. (Oxford: Oxford University Press), pp. 153-179.

Bereiter-Hahn, J., and Voth, M. (1994). Dynamics of mitochondria in living cells: shape changes, dislocations, fusion, and fission of mitochondria. Microsc Res Tech 27, 198-219.

Bleazard, W., McCaffery, J. M., King, E. J., Bale, S., Mozdy, A., Tieu, Q., Nunnari, J., and Shaw, J. M. (1999). The dynamin-related GTPase Dnm1 regulates mitochondrial fission in yeast. Nature Cell Biol. 1, 298 - 304.

Boldogh, I., Vojtov, N., Karmon, S., and Pon, L. A. (1998). Interaction between mitochondria and the actin cytoskeleton in budding yeast requires two integral mitochondrial outer membrane proteins, Mmm1p and Mdm10p. J Cell Biol 141, 1371-81.

Chien, C.-T., Bartel, P. L., Sternglanz, R., and Fields, S. (1991). The two-hybrid system: a method to identify and clone genes for proteins that interact with a protein of interest. Proc. Natl. Acad. Sci. USA 88, 9578-9582.

Collins, T. J., Berridge, M. J., Lipp, P., and Bootman, M. D. (2002). Mitochondria are morphologically and functionally heterogeneous within cells. Embo J 21, 1616-27.

Danino, D., and Hinshaw, J. E. (2001). Dynamin family of mechanoenzymes. Curr Opin Cell Biol 13, 454-60.

De Giorgi, F., Lartigue, L., and Ichas, F. (2000). Electrical coupling and plasticity of the mitochondrial network. Cell Calcium 28, 365-70.

Desagher, S., and Martinou, J. C. (2000). Mitochondria as the central control point of apoptosis. Trends Cell Biol. 10, 369-377.

Enriquez, J. A., Cabezas-Herrera, J., Bayona-Bafaluy, M. P., and Attardi, G. (2000). Very rare complementation between mitochondria carrying different mitochondrial DNA

mutations points to intrinsic genetic autonomy of the organelles in cultured human cells. J. Biol. Chem. 275, 11207-11215.

Frank, S., Gaume, B., Bergmann-Leitner, E. S., Leitner, W. W., Robert, E. G., Catez, F., Smith, C. L., and Youle, R. J. (2001). The role of dynamin-related protein 1, a mediator of mitochondrial fission, in apoptosis. Dev Cell 1, 515-25.

Fritz, S., Rapaport, D., Klanner, E., Neupert, W., and Westermann, B. (2001). Connection of the mitochondrial outer and inner membranes by Fzo1 is critical for organellar fusion. J. Cell Biol. 152, 683-92.

Futatsugi, N., and Tsuda, M. (2001). Molecular dynamics simulations of Gly-12-->Val mutant of p21(ras): dynamic inhibition mechanism. Biophys J 81, 3483-8.

Griparic, L., and van der Bliek, A. M. (2001). The many shapes of mitochondrial membranes. Traffic 2, 235-44.

Guo, W., Roth, D., Walch-Solimena, and Novick, P. (1999). The exocyst is an effector for Sec4p, targeting secretory vesicle to sites of exocytosis. EMBO J. 18, 1071-1080.

Haas, A., Scheglmann, D., Lazar, T., Gallwitz, D., and Wickner, W. (1995). The GTPase Ypt7p of Saccharomyces ceerevisiae is required on both partner vacuoles for the homotypic fusion step of vacuole inheritance. EMBO J. 14, 5258-5270.

Hales, K. G., and Fuller, M. T. (1997). Developmentally regulated mitochondrial fusion mediated by a conserved, novel, predicted GTPase. Cell 90, 121-129.

Hayashi, J., Takemitsu, M., Goto, Y., and Nonaka, I. (1994). Human mitochondria and mitochondrial genome function as a single dynamic cellular unit. J. Cell Biol. 125, 43-50.

Hermann, G. J., and Shaw, J. S. (1998a). Mitochondrial dynamics in yeast. Annu. Rev. Cell Dev. Biol. 14, 265-303.

Hermann, G. J., Thatcher, J. W., Mills, J. P., Hales, K. G., Fuller, M. T., Nunnari, J., and Shaw, J. M. (1998b). Mitochondrial fusion in yeast requires the transmembrane GTPase Fzo1p. J. Cell Biol. 143, 359-373.

Huser, J., and Blatter, L. A. (1999). Fluctuations in mitochondrial membrane potential caused by repetitive gating of the permeability transition pore. Biochem J 343, 311-7.

Hwa, J. J., Hiller, M. A., Fuller, M. T., and Santel, A. (2002). Differential expression of the Drosophila mitofusin genes fuzzy onions (fzo) and dmfn. Mech Dev 116, 213-6.

Jagath, J. R. Rodnina, M. V. Lentzen, G. Wintermeyer, W. (1998). Interaction of guanine nucleotides with the signal recognition particle from Escherichia coli. Biochemistry 44, 15408-13.

Jones, S., Newman, C., Liu, F., and Segev, N. (2000). The TRAPP complex is a nucleotide exchanger for Ypt1 and Ypt31/32. Mol Biol Cell 11, 4403-11.

Karbowski, M., Lee, Y. J., Gaume, B., Jeong, S. Y., Frank, S., Nechushtan, A., Santel, A., Fuller, M., Smith, C. L., and Youle, R. J. (2002). Spatial and temporal association of Bax with mitochondrial fission sites, Drp1, and Mfn2 during apoptosis. J Cell Biol 159, 931-8.

Knott, T. G., Birdsey, G. M., Sinclair, K. E., Gallagher, I. M., Purdue, P. E., and Danpure, C. J. (2000). The peroxisomal targeting sequence type 1 receptor, Pex5p, and the peroxisomal import efficiency of alanine:glyoxylate aminotransferase. Biochem J 352, 409-18.

Krengel, U.Schlichting, I.Scherer, A.Schumann, R.Frech, M.John, J.Kabsch, W.Pai, E.F,Wittinghofer, A. (1990). Three dimensional structure of H-ras p21 mutants: molecular basis for their inability to function as signal switch molecules Cell 62, 539-48

Labrousse, A. M., Zappaterra, M. D., Rube, D. A., and van der Bliek, A. M. (1999). C. elegans dynamin-related protein DRP-1 controls severing of the mitochondrial outer membrane. Mol. Cell. 4, 815-826.

Lee, S. S., Lee, R. Y., Fraser, A. G., Kamath, R. S., Ahringer, J., and Ruvkun, G. (2003). A systematic RNAi screen identifies a critical role for mitochondria in C. elegans longevity. Nat Genet 33, 40-8.

Legros, F.Lombes, A.Frachon, P.Rojo, M. (2002). Mitochondrial fusion in human cells is efficient, requires the inner membrane potential, and is mediated by mitofusins. Mol Biol Cell 13, 4343-54.

Mandiyan, V., Andreev, J., Schlessinger, J., and Hubbard, S. R. (1999). Crystal structure of the ARF-GAP domain and ankyrin repeats of PYK2-associated protein beta. Embo J 18, 6890-8.

Mayer, A., and Wickner, W. (1997). Docking of yeast vacuoles is catalyzed by the Ras-like GTPase Ypt7p after symmetric priming by Sec18p (NSF). J. Cell Biol. 136, 307-317.

McBride, H. M., Rybin, V., Murphy, C., Giner, A., Teasdale, R., and Zerial, M. (1999). Oligomeric complexes link Rab5 effectors with NSF and drive membrane fusion via interactions between EEA1 and syntaxin 13. Cell 98, 377-386.

Nakada, K., Inoue, K., Ono, T., Isobe, K., Ogura, A., Goto, Y. I., Nonaka, I., and Hayashi, J. I. (2001). Inter-mitochondrial complementation: Mitochondria-specific system preventing mice from expression of disease phenotypes by mutant mtDNA. Nat. Med. 7, 934-940.

Nakamura, N., Lowe, M., Levine, T. P., Rabouille, C., and Warren, G. (1997). The vesicle docking protein p115 binds GM130, a cis-Golgi matrix protein, in a mitotically regulated manner. Cell 89, 445-455.

Nangaku, M., Sato-Yoshitake, R., Okada, Y., Noda, Y., Takemura, R., Yamazaki, H., and Hirokawa, N. (1994). KIF1B, a novel microtubule plus end-directed monomeric motor protein for transport of mitochondria. Cell, 1209-1220.

Novick, P., and Brennwald, P. (1993). Friends and family: The role of the Rab GTPases in vesicular transport. Cell 75, 597-601.

Novick, P., and Zerial, M. (1997). The diversity of Rab proteins in vesicle transport. Curr. Opin. Cell Biol. 9, 496-504.

Okamoto, K., Perlman, P. S., and Butow, R. A. (1998). The sorting of mitochondrial DNA and mitochondrial proteins in zygotes: preferential transmission of mitochondrial DNA to the medial bud. J Cell Biol 142, 613-23.

Ono, T., Isobe, K., Nakada, K., and Hayashi, J. I. (2001). Human cells are protected from mitochondrial dysfunction by complementation of DNA products in fused mitochondria. Nat. Genet. 28, 272-275.

Otsuga, D., Keegan, B. R., Brisch, E., Thatcher, J. W., Hermann, G. J., Bleazard, W., and Shaw, J. M. (1998). The dynamin-related GTPase, Dnm1p, controls mitochondrial morphology in yeast. J. Cell Biol. 143, 333-349.

Prakash, B., Praefcke, G. J., Renault, L., Wittinghofer, A., and Herrmann, C. (2000). Structure of human guanylate-binding protein 1 representing a unique class of GTP-binding proteins. Nature 403, 567-571.

Price, A., Seals, D., Wickner, W., and Ungermann, C. (2000). The docking stage of yeast vacuole fusion requires the transfer of proteins from a cis-SNARE complex to a Rab/Ypt protein. J Cell Biol 148, 1231-8.

Radi, R., Turrens, J. F., Chang, L. Y., Bush, K. M., Crapo, J. D., and Freeman, B. A. (1991). Detection of catalase in rat heart mitochondria. J Biol Chem 266, 22028-34.

Rak, A., Fedorov, R., Alexandrov, K., Albert, S., Goody, R. S., Gallwitz, D., and Scheidig, A. J. (2000). Crystal structure of the GAP domain of Gyp1p: first insights into interaction with Ypt/Rab proteins. Embo J 19, 5105-13.

Ranger, A. M., Malynn, B. A., and Korsmeyer, S. J. (2001). Mouse models of cell death. Nat Genet 28, 113-8.

Rapaport, D., Brunner, M., Neupert, W., and Westerman, B. (1998). Fzo1p is a mitochondrial outer membrane protein essential for the biogenesis of functional mitochonrdia in Saccharomyces cerevisiae. J. Biol. Chem. 273, 20150-20155.

Reichert, A. S., and Neupert, W. (2002). Contact sites between the outer and inner membrane of mitochondria-role in protein transport. Biochim Biophys Acta 1592, 41-9.

Resat, H., Straatsma, T. P., Dixon, D. A., and Miller, J. H. (2001). The arginine finger of RasGAP helps Gln-61 align the nucleophilic water in GAP-stimulated hydrolysis of GTP. Proc Natl Acad Sci U S A 98, 6033-8.

Richter, M. F., Schwemmle, M., Herrmann, C., Wittinghofer, A., and Staeheli, P. (1995). Interferon-induced MxA protein. GTP binding and GTP hydrolysis properties. J Biol Chem 270, 13512-7.

Rittinger, K., Walker, P. A., Eccleston, J. F., Smerdon, S. J., and Gamblin, S. J. (1997). Structure at 1.65 A of RhoA and its GTPase-activating protein in complex with a transition-state analogue. Nature 389, 758-62.

Rojo, M., Legros, F., Chateau, D., and Lombes, A. (2002). Membrane topology and mitochondrial targeting of mitofusins, ubiquitous mammalian homologs of the transmembrane GTPase Fzo. J Cell Sci 115, 1663-74.

Rothman, J. E., and Sollner, T.H. (1997). Throttles and dampers: controlling the engine of membrane fusion. Science 276, 1212-1213.

Rothman, J. E., and Warren, G. (1994). Implications of the SNARE hypothesis for intracellular membrane topology and dynamics. Current Biology 4, 220-233.

Rybin, V., Ullrich, O., Rubino, M., Alexandrov, K., Simon, I., Seabra, M. C., Goody, R., and Zerial, M. (1996). GTPase activity of rab5 acts as a timer for endocytic membrane fusion. Nature 383, 266-269.

Sacher, M., Jiang, Y., Barrowman, J., Scarpa, A., Burston, J., Zhang, L., Schieltz, D., Yates, J.R., Abeliovich, H., and Ferro-Novick, S. (1998). TRAPP, a highly conserved novel complex on the cis-Golgi that mediates vesicle docking and fusion. EMBO J 17, 2494-2503.

Santel, A., and Fuller, M. T. (2001). Control of mitochondrial morphology by a human mitofusin. J. Cell Sci. 114, 867-874.

Saraste, M. (1999). Oxidative phosphorylation at the fin de siecle. Science 283, 1488-93.

Scheidig, A. J., Franken, S. M., Corrie, J. E., Reid, G. P., Wittinghofer, A., Pai, E. F., and Goody, R. S. (1995). X-ray crystal structure analysis of the catalytic domain of the oncogene product p21H-ras complexed with caged GTP and mant dGppNHp. J Mol Biol 253, 132-50.

Schroer, T. A., Steuer, E. R., and Sheetz, M. P. (1989). Cytoplasmic dynein is a minus end-directed motor for membranous organelles. Cell 56, 937-946.

Seals, D. F., Eitzen, G., Margolis, N., Wickner, W. T., and Price, A. (2000). A Ypt/Rab effector complex containing the Sec1 homolog Vps33p is required for homotypic vacuole fusion. Proc Natl Acad Sci U S A 97, 9402-7.

Serebriiskii, I., Estojak, J., Berman, M., and Golemis, E. A. (2000). Approaches to detecting false positives in yeast two-hybrid systems. Biotechniques 28, 328-30, 332-6.

Sesaki, H., and Jensen, R. E. (1999). Division versus Fusion: Dnm1p and Fzo1p Antagonistically Regulate Mitochondrial Shape. J Cell Biol 147, 699-706.

Simon, V. R., Karmon, S. L., and Pon, L. A. (1997). Mitochondrial inheritance: cell cycle and actin cable dependence of polarized mitochondrial movements in Saccharomyces cerevisiae. Cell Motil. Cytoskeleton 37, 199-210.

Smirnova, E., Griparic, L., Shurland, D. L., and van Der Bliek, A. M. (2001). Dynamin-related protein drp1 is required for mitochondrial division in mammalian cells. Mol Biol Cell 12, 2245-2256.

Sollner, T. H. (2002). Vesicle tethers promoting fusion machinery assembly. Dev Cell 2, 377-8.

Song, B. D., and Schmid, S. L. (2003). A Molecular Motor or a Regulator? Dynamin's in a Class of Its Own. Biochemistry 42, 1369-76.

Stocco, D. M. (2001). StAR protein and the regulation of steroid hormone biosynthesis. Annu Rev Physiol 63, 193-213

Takai, D., Isobe, K., and Hayashi, J. (1999). Transcomplementation between different types of respiration-deficient mitochondria with different pathogenic mutant mitochondrial DNAs. J. Biol. Chem. 274, 11199-202.

Tanaka, Y., Kanai, Y., Okada, Y., Nonaka, S., Takeda, S., Harada, A., and Hirokawa, N. (1998). Targeted disruption of mouse conventional kinesin heavy chain, kif5B, results in abnormal perinuclear clustering of mitochondria. Cell 93, 1147-1158.

TerBush, D. R., Maurice, T., Roth, D., and Novick, P. (1996). The exocyst is a multiprotein complex required for exocytosis in Saccharomyces cerevisae. EMBO J 15, 6483-6494.

Tong, L. A., de Vos, A. M., Milburn, M. V., Jancarik, J., Noguchi, S., Nishimura, S., Miura, K., Ohtsuka, E., and Kim, S. H. (1989). Structural differences between a ras oncogene protein and the normal protein. Nature 337, 90-3.

Vetter, I. R., and Wittinghofer, A. (2001). The guanine nucleotide-binding switch in three dimensions. Science 294, 1299-304.

Wallace, D. C. (1999). Mitochondrial diseases in man and mouse. Science 283, 1482-1488.

Wang, W., Sacher, M., and Ferro-Novick, S. (2000). TRAPP stimulates guanine nucleotide exchange on Ypt1p. J Cell Biol 151, 289-96.

Weber, T., Zemelman, B. V., McNew, J. A., Westermann, B., Gmachl, M., Parlati, F., Solner, T., and Rothman, J. E. (1998). SNAREpins: Minimal machinery for membrane fusion. Cell 92, 759-772.

Weimbs, T., Low, S. H., Chapin, S. J., Mostov, K. E., Bucher, P., and Hofmann, K. (1997). A conserved domain is present in different families of vesicular fusion proteins: a new superfamily. Proc Natl Acad Sci U S A 94, 3046-51.

Yaffe, M. P. (1999). Dynamic mitochondria. Nat. Cell Biol. 1, E149-50.

Zamzami, N., and Kroemer, G. (2001). The mitochondrion in apoptosis: how Pandora's box opens. Nat Rev Mol Cell Biol 2, 67-71.

Zerial, M., and McBride, H. (2001). Rab proteins as membrane organizers. Nat Rev Mol Cell Biol 2, 107-17.

Zerial, M., and Stenmark, H. (1993). Rab GTPases in vesicular transport. Cur. Op. Cell Biol. 5, 613-620.

SUPPLEMENTAL VIDEOS ON A COMPACT DISC

1. Figure 14, Movie 1
2. Figure 20, Movie 1
3. Figure 20, Movie 2
4. Figure 20, Movie 3
5. Figure 20, Movie 4
6. Figure 20, Movie 5